

# No-regret Algorithms for Multi-task Bayesian Optimization

Sayak Ray Chowdhury    Aditya Gopalan  
Indian Institute of Science

November 7, 2021

## Abstract

We consider multi-objective optimization (MOO) of an unknown vector-valued function in the non-parametric Bayesian optimization (BO) setting, with the aim being to learn points on the Pareto front of the objectives. Most existing BO algorithms do not model the fact that the multiple objectives, or equivalently, tasks can share similarities, and even the few that do lack rigorous, finite-time regret guarantees that capture explicitly inter-task structure. In this work, we address this problem by modelling inter-task dependencies using a multi-task kernel and develop two novel BO algorithms based on random scalarizations of the objectives. Our algorithms employ vector-valued kernel regression as a stepping stone and belong to the upper confidence bound class of algorithms. Under a smoothness assumption that the unknown vector-valued function is an element of the reproducing kernel Hilbert space associated with the multi-task kernel, we derive worst-case regret bounds for our algorithms that explicitly capture the similarities between tasks. We numerically benchmark our algorithms on both synthetic and real-life MOO problems, and show the advantages offered by learning with multi-task kernels.

## 1 Introduction

Bayesian optimization is a popular approach for optimizing a black-box function with expensive, noisy evaluations, having been extensively applied in various applications such as hyper-parameter tuning (Snoek et al., 2012), sensor selection (Garnett et al., 2010), synthetic gene design (Gonzalez et al., 2015), etc. In many practical scenarios, one is required to optimize *multiple* objectives together, and moreover, these objectives can be conflicting in nature. For example, consider drug discovery, where each function evaluation is a costly laboratory experiment and its output is a measurement of both the potency and side-effects of a candidate drug (Paria et al., 2019). These two objectives are typically conflicting in nature, since one would like to maximize the potency of drug while also keeping its side-effects to a minimum. Other examples include tradeoffs such as bias and variance, accuracy and calibration (Guo et al., 2017), accuracy and fairness (Zliobaite, 2015) etc. These problems can be framed as that of optimizing a vector-valued function  $f = (f_1, \dots, f_n)$ , where each of its components is a real-valued

function and corresponds to a particular objective or task. Since one often cannot optimize all  $f_i$ 's simultaneously, most multi-objective optimization (MOO) approaches aim to recover the set of Pareto optimal points, where intuitively a point is Pareto optimal if there is no way to improve on all objectives simultaneously (Knowles, 2006; Ponweiser et al., 2008). Popular BO strategies in this regard include Predictive Entropy Search (Hernández-Lobato et al., 2016), max-value entropy search (Belakaria et al., 2019), Pareto active learning (Zuluaga et al., 2013), expected hypervolume improvement (Emmerich and Klinkenberg, 2008), sequential uncertainty reduction (Picheny, 2015) and scalarization based approaches (Rojers et al., 2013). Random scalarizations, in particular, have been shown to be flexible enough to model user preferences in capturing the whole or a part of the *Pareto front* (Paria et al., 2019).

Most multi-objective BO approaches maintain  $n$  different Gaussian processes (GPs) (Rasmussen, 2003), one for each task or objective  $f_i$ . However, in general, the tasks share some underlying structure, and cannot be treated as unrelated objects. By making use of this structure, one might benefit significantly by learning the tasks simultaneously as opposed to learning them independently. For example, consider predicting consumer preferences simultaneously based on their past history (Evgeniou et al., 2005). Each task is to learn the preference of a particular consumer, and the tasks are related since people with similar tastes tend to buy similar items. Other examples include simultaneous estimation of many related indicators in economic forecasting (Greene, 2003), predicting tumour behaviour from multiple related diseases (Rifkin et al., 2003) etc. However, assuming similarities in a set of tasks and blindly learning them together can be detrimental (Caruana, 1997). Hence, it is important to have a model that will benefit the learning in case of related tasks and will not hurt performance when the tasks are unrelated. This can be achieved by maintaining a *multi-task* GP over  $f$ , which directly induces correlations between tasks (Bonilla et al., 2008). In the context of BO, Swersky et al. (2013) empirically demonstrate the utility of this model in a number of applications, and Astudillo and Frazier (2019) provide an asymptotic convergence analysis under a special setting of composite objective functions and noise-free evaluations. However, a formal finite time regret analysis showing the effectiveness of multi-task GPs over independent GPs in the context of noisy MOO has not been rigorously pursued. Against this backdrop, we make the following contributions:

- We develop two novel BO algorithms – multi-task kernelized bandits (MT-KB) and multi-task budgeted kernelized bandits (MT-BKB) – that are based on random scalarizations, and can leverage similarities between tasks to optimize them more efficiently.
- Our algorithms use vector-valued kernel ridge regression as a building block and follow the general template of the upper-confidence-bound class of algorithms. Also, MT-BKB is the first algorithm that employs the *Nyström approximation* in the context of *multi-task kernels*.
- Under the assumption that the objective function has smoothness compatible with a joint kernel on its domain and components, we derive (scalarization induced) regret bounds for our algorithms that *explicitly capture the inter-task structure*. These are the first worst-case (frequentist) regret bounds for multi-objective BO,

and are proved by deriving a novel concentration inequality for the estimate of the vector-valued objective function, which might be of independent interest.

- Finally, our algorithms are simple to implement when the kernel decouples between tasks and domain, and we report numerical results on synthetic as well as real-world based datasets, for which the algorithms are seen to perform favourably.

**Related work.** In the field of geostatistics (Wackernagel, 2013), and more recently in supervised learning (Liu et al., 2018), multi-task GPs and associated kernels have gained a lot of traction. Also, a lot of work has been done in the context of vector-valued learning with kernel methods (Micchelli and Pontil, 2005; Baldassarre et al., 2012; Grünewälder et al., 2012), and this paper complements the literature by considering an online learning setting. A simple version of multi-objective black box optimization – in the form of online learning in finite multi-armed bandits (MABs) – has been considered in (Drugan and Nowe, 2013; Drugan and Nowé, 2014). This paper, in effect, generalize these works to the more challenging setting of infinite-armed bandits, which has been studied extensively in the single task setting (Srinivas et al., 2010; Chowdhury and Gopalan, 2017; Scarlett et al., 2017).

## 2 Problem statement

We consider the problem of maximizing a vector-valued function  $f(x) = [f_1(x), \dots, f_n(x)]^\top$  over a compact domain  $\mathcal{X} \subset \mathbb{R}^d$ . At each round  $t$ , a learner queries  $f$  at a single point  $x_t \in \mathcal{X}$ , and observes a noisy output  $y_t = f(x_t) + \varepsilon_t$ , where  $\varepsilon_t \in \mathbb{R}^n$  is a zero-mean *sub-Gaussian* random vector conditioned on  $\mathcal{F}_{t-1}$ , the  $\sigma$ -algebra generated by the random variables  $\{x_s, \varepsilon_s\}_{s=1}^{t-1}$  and  $x_t$ . By this we mean that there exists a  $\sigma \geq 0$ , such that

$$\forall \alpha \in \mathbb{R}^n, \forall t \geq 1, \quad \mathbb{E} [\exp(\alpha^\top \varepsilon_t) \mid \mathcal{F}_{t-1}] \leq \exp(\sigma^2 \|\alpha\|_2^2 / 2).$$

The query point  $x_t$  at round  $t$  is chosen causally depending upon the history  $\{(x_s, y_s)\}_{s=1}^{t-1}$  of query and output sequences available up to round  $t-1$ . Since one cannot optimize all  $f_i$ 's simultaneously, the learner's aim is to find the set of *Pareto-optimal* points, denoted by  $\mathcal{X}_f$ . A point  $x$  is said to be Pareto dominated by  $x'$  if  $f(x) \prec f(x')$ , where for any  $u, v \in \mathbb{R}^n$ ,  $u \prec v$  denotes that  $u_i \leq v_i$  for all  $i \in [n]$  and  $u_j < v_j$  for some  $j \in [n]$ .<sup>1</sup> A point is Pareto optimal if it is not Pareto dominated by any other points, i.e.,  $x \in \mathcal{X}_f$  if  $f(x) \not\prec f(x')$  for all  $x' \neq x$ . The *Pareto front* of  $f$  is denoted by  $f(\mathcal{X}_f)$ , where for any set  $\mathcal{A}$ ,  $f(\mathcal{A}) := \{f(x) \mid x \in \mathcal{A}\}$ .

**Random scalarizations and Pareto optimality** A common approach to solve the multi-objective optimization problem is by converting the objective vectors  $f(x)$  into single objective scalars using a *scalarization function*  $s_\lambda : \mathbb{R}^n \rightarrow \mathbb{R}$ , parameterized by a weight vector  $\lambda \in \Lambda \subset \mathbb{R}^n$ . Similar to Paria et al. (2019), we assume random scalarizations, i.e., access to a (known) distribution  $P_\lambda$  with its support on  $\Lambda$ . Thus, instead of maximizing a single scalarized objective, we aim to maximize over a set of

<sup>1</sup>We denote by  $[n]$  the set  $\{1, 2, \dots, n\}$ .

scalarizations weighted by the distribution  $P_\lambda$ . (Note that the Dirac-delta distribution  $P_\lambda^2$  yields a deterministic scalarization.) We also assume that, for all  $\lambda$ , the scalarization function  $s_\lambda$  is  $L_\lambda$ -Lipschitz in the  $\ell_2$ -norm, i.e.,

$$\forall u, v \in \mathbb{R}^n, \quad |s_\lambda(u) - s_\lambda(v)| \leq L_\lambda \|u - v\|_2.$$

Commonly used scalarization functions include the linear scalarization  $s_\lambda(y) = \sum_{i=1}^n \lambda_i y_i$  and the Chebyshev scalarization  $s_\lambda(y) = \min_{i \in [n]} \lambda_i (y_i - z_i)$ , where  $z \in \mathbb{R}^n$  is a reference point and  $\lambda$  lies in the set  $\Lambda = \{\lambda \succ 0 : \|\lambda\|_1 = 1\}$  (Nakayama et al., 2009). Apart from being Lipschitz, another important property these scalarizations have is monotonicity in all co-ordinates, i.e.,  $s_\lambda(u) < s_\lambda(v)$  whenever  $u \prec v$ . Monotonicity ensures that  $x_\lambda^* := \operatorname{argmax}_{x \in \mathcal{X}} s_\lambda(f(x))$ , the maximizer of the scalarized objective, is a Pareto optimal point, since otherwise if  $f(x_\lambda^*) \prec f(x)$  for some  $x \neq x_\lambda^*$ , we have  $s_\lambda(f(x_\lambda^*)) < s_\lambda(f(x))$  yielding a contradiction. Therefore,  $P_\lambda$  defines a probability distribution over the Pareto optimal set  $\mathcal{X}_f$ , and thus, in turn, over the Pareto front  $f(\mathcal{X}_f)$ . Hence, the distribution  $P_\lambda$  provides flexibility to sample from the entire or a part of the Pareto front depending on the application (Paria et al., 2019).

**Performance metric** Given a budget of  $T$  rounds, our goal is to find a set  $\mathcal{X}_T := \{x_1, \dots, x_T\} \subset \mathcal{X}$  such that  $f(\mathcal{X}_T)$  well approximates the high probability regions of the Pareto front  $f(\mathcal{X}_f)$ . This can be achieved, as shown in Paria et al. (2019), by minimizing the *Bayes regret*, defined as

$$R_B(T) = \mathbb{E}_{P_\lambda} [r_\lambda(T)], \quad \text{where } r_\lambda(T) = s_\lambda(f(x_\lambda^*)) - \max_{x \in \mathcal{X}_T} s_\lambda(f(x)).$$

To see this, we note that it requires  $r_\lambda(T)$  to be low for all  $\lambda \in \Lambda$  that has high mass, to achieve a low Bayes regret. Now, by definition,  $r_\lambda(T) = 0$  if  $x_\lambda^* \in \mathcal{X}_T$ , and also, by monotonicity,  $x_\lambda^* \in \mathcal{X}_f$ . Then, by the Lipschitz continuity, a low value of  $R_B(T)$  will essentially imply  $f(\mathcal{X}_T)$  to "span" the high probability regions of  $f(\mathcal{X}_f)$ . A more classical performance measure is the (scalarized) *cumulative regret*

$$R_C(T) = \sum_{t=1}^T \mathbb{E}_{P_\lambda} [s_{\lambda_t}(f(x_{\lambda_t}^*)) - s_{\lambda_t}(f(x_t))],$$

where each  $\lambda_t$  is independent and  $P_\lambda$  distributed. If  $\Lambda$  is a bounded set and the scalarization  $s_\lambda$  is also Lipschitz in  $\lambda$ , then one can show that  $R_B(T) \leq \frac{1}{T} R_C(T) + o(1)$  (Paria et al., 2019). A sub-linear growth of  $R_C(T)$  with  $T$  then implies that  $R_B(T) \rightarrow 0$  as  $T \rightarrow \infty$ .

**Regularity assumptions** Attaining non-trivial regret bound is impossible in general for arbitrary vector-valued functions  $f$ , thus some regularity assumptions are in order. We call a mapping  $\Gamma : \mathcal{X} \times \mathcal{X} \rightarrow \mathbb{R}^{n \times n}$ , a *multi-task kernel*<sup>3</sup> on  $\mathcal{X}$  if  $\Gamma(x, x')^\top =$

<sup>2</sup>A Dirac-delta is a probability distribution that puts mass 1 on exactly one point in the probability space.

<sup>3</sup>In its more general form, this definition can be lifted from  $\mathbb{R}^n$  to any arbitrary Hilbert space  $\mathcal{H}$  (Caponnetto et al., 2008).

$\Gamma(x', x)$  for any  $x, x' \in \mathcal{X}$ , and it is positive definite, i.e., for any  $m \in \mathbb{N}$ ,  $\{x_i\}_{i=1}^m \subseteq \mathcal{X}$  and  $\{y_i\}_{i=1}^m \subseteq \mathbb{R}^n$  it holds

$$\sum_{i,j=1}^m y_i^\top \Gamma(x_i, x_j) y_j \geq 0 .$$

Given a continuous (relative to the induced matrix norm) multi-task kernel  $\Gamma$  on  $\mathcal{X}$ , there exists a unique (modulo an isometry) vector-valued reproducing kernel Hilbert space (RKHS) of vector-valued continuous functions  $g : \mathcal{X} \rightarrow \mathbb{R}^n$ , with  $\Gamma$  as its reproducing kernel (Carmeli et al., 2010). We denote this RKHS as  $\mathcal{H}_\Gamma(\mathcal{X})$ , with the corresponding inner product  $\langle \cdot, \cdot \rangle_\Gamma$ . Then, for every  $x \in \mathcal{X}$ , there exists a bounded linear operator  $\Gamma_x : \mathbb{R}^n \rightarrow \mathcal{H}_\Gamma(\mathcal{X})$  such that the following holds:

$$\forall x' \in \mathcal{X}, \quad \Gamma(x, x') = \Gamma_x^\top \Gamma_{x'} \quad \text{and} \quad \forall g \in \mathcal{H}_\Gamma(\mathcal{X}), \quad g(x) = \Gamma_x^\top g .$$

Here,  $\Gamma_x^\top$  denotes the adjoint of  $\Gamma_x$  (with a slight abuse of notation), and it is the unique operator that satisfies the following:

$$\forall g \in \mathcal{H}_\Gamma(\mathcal{X}), \quad \forall y \in \mathbb{R}^n, \quad \langle \Gamma_x^\top g, y \rangle_2 = \langle g, \Gamma_x y \rangle_\Gamma .$$

We assume that the objective function  $f$  is an element of the RKHS  $\mathcal{H}_\Gamma(\mathcal{X})$  and its norm associated to  $\mathcal{H}_\Gamma(\mathcal{X})$  is bounded, i.e., there exists a  $b < \infty$  such that  $\|f\|_\Gamma \leq b$ . This is a measure of smoothness of  $f$ , since, by the reproducing property

$$\forall x, x' \in \mathcal{X}, \quad \|f(x) - f(x')\|_2 \leq \|f\|_\Gamma \|\Gamma_x - \Gamma_{x'}\| ,$$

where  $\|\Gamma_x\| := \sup_{\|y\|_2 \leq 1} \|\Gamma_x y\|_\Gamma$  denotes the operator norm. Further, we assume that there exists a  $\kappa < \infty$  such that  $\|\Gamma(x, x)\| \leq \kappa$  for all  $x \in \mathcal{X}$ . Note that in the single-task setting ( $n = 1$ ), the kernel  $\Gamma$  is scalar-valued and the RKHS  $\mathcal{H}_\Gamma(\mathcal{X})$  consists of real-valued functions. In this case, the bounded norm assumption holds for stationary kernels, e.g., the *squared exponential* (SE) kernel and the *Matérn* kernel (Srinivas et al., 2010; Chowdhury and Gopalan, 2017).

**Examples of multi-task (MT) kernels** It is possible to construct MT kernels using scalar kernels  $k : \mathcal{X} \times \mathcal{X} \rightarrow \mathbb{R}^+$ . Evgeniou et al. (2005) consider the kernel

$$\Gamma(x, x') = k(x, x') (\omega I_n + (1 - \omega) 1_n/n) ,$$

where  $I_n$  is the  $n \times n$  identity matrix,  $1_n$  is the  $n \times n$  all-one matrix and  $\omega \in [0, 1]$  is a parameter that governs the similarity level between components of  $f$ . The choice  $\omega = 1$  corresponds to assuming that all tasks are unrelated and possible similarity among them is not exploited. Conversely,  $\omega = 0$  is equivalent to assuming that all tasks are identical and can be explained by the same function. Swersky et al. (2013) consider a more general class of kernels known as the *intrinsic coregionalization model* (ICM), which includes the aforementioned kernel as a special case. The kernels are of the form

$$\Gamma(x, x') = k(x, x') B ,$$

where  $B$  is an  $n \times n$  p.s.d. matrix that encodes the inter-task structure. This class of kernels is called *separable* since it allows to decouple the contribution of input and output in the covariance structure (Alvarez et al., 2011). We consider stationary scalar kernels  $k$  with unit variances – to avoid redundancy in the parameterization – since the variances can be captured fully by  $B$  (Bonilla et al., 2008). The main advantage of ICM is that one can use the eigen-system of  $B$  to define a new coordinate system where  $\Gamma$  becomes block diagonal, reducing the computational burden to a great extent. The diagonal MT kernel  $\Gamma(x, x') = \text{diag}(k_1(x, x'), \dots, k_n(x, x'))$  has the same advantage, but corresponds to treating each task independently using different scalar kernels  $k_j$ . However, in general, a MT kernel will not be diagonal, and moreover cannot be reduced to a diagonal one by linearly transforming the output space. For example, it is impossible to reduce the kernel  $\Gamma(x, x') = \sum_{j=1}^M k_j(x, x') B_j$ ,  $M \neq 1$ , to a diagonal one, unless all the  $n \times n$  matrices  $B_j$  are simultaneously diagonalizable (Caponnetto et al., 2008).

### 3 Our approach

We follow the general template of upper confidence bound (UCB) class of BO algorithms (Srinivas et al., 2010; Chowdhury and Gopalan, 2017) suitably adapted to the multi-task setting. At each round  $t$ , we randomly sample a weight vector  $\lambda_t$  from the distribution  $P_\lambda$ , and compute a multi-task acquisition function  $u_t : \mathcal{X} \rightarrow \mathbb{R}$  to act as an UCB for the unknown function  $f$ , based on the random scalarization  $s_{\lambda_t}$ . Whenever  $u_t(x)$  is a valid UCB, i.e.,  $s_{\lambda_t}(f(x)) \leq u_t(x)$ , and it converges to  $s_{\lambda_t}(f(x))$  “sufficiently” fast, then selecting candidates that are optimal with respect to  $u_t$  leads to low (scalarized) regret, i.e., the scalarized objective  $s_{\lambda_t}(f(x_t))$  at  $x_t \in \text{argmax}_{x \in \mathcal{X}} u_t(x)$  tends to  $s_{\lambda_t}(f(x_{\lambda_t}^*))$  as  $t$  increases. The intuition behind our approach, at a high level, is that the set  $f(\mathcal{X}_t)$  tends to the high probability regions of the Pareto front as  $t$  increases. It now remains to design a principled multi-task acquisition function  $u_t$  based on the scalarization  $s_{\lambda_t}$ , and in what follows, we shall describe two algorithms for that.

#### 3.1 Algorithm 1: Multi-task kernelized bandits (MT-KB)

Given the data  $\{(x_i, y_i)\}_{i=1}^t \subset \mathcal{X} \times \mathbb{R}^n$ , we first aim to find an estimate of  $f$  by solving a vector-valued regression problem:

$$\min_{f \in \mathcal{H}_\Gamma(\mathcal{X})} \sum_{i=1}^t \|y_i - f(x_i)\|_2^2 + \eta \|f\|_\Gamma^2 ,$$

where  $\eta > 0$  is a regularizing parameter. Micchelli and Pontil (2005) show that the solution of this minimization problem can be written as

$$\mu_t = \sum_{i=1}^t \Gamma_{x_i} \alpha_i .$$

Here,  $\{\alpha_i\}_{i=1}^t \subseteq \mathbb{R}^n$  is the unique solution of the linear system of equations

$$\sum_{i=1}^t (\Gamma(x_j, x_i) + \eta \delta_{j,i}) \alpha_i = y_j, \quad 1 \leq j \leq t,$$

where  $\delta_{j,i}$  denotes the Kronecker-delta function. Now, by the reproducing property, we have

$$\mu_t(x) = \Gamma_x^\top \mu_t = G_t(x)^\top (G_t + \eta I_{nt})^{-1} Y_t,$$

where the kernel matrix  $G_t = [\Gamma(x_i, x_j)]_{i,j=1}^t$  is a  $t \times t$  block matrix with each block being an  $n \times n$  matrix (so that  $G_t$  is an  $nt \times nt$  matrix),  $Y_t = [y_1^\top, \dots, y_t^\top]^\top$  is an  $nt \times 1$  vector with the outputs concatenated, and  $G_t(x) = [\Gamma(x, x_1)^\top, \dots, \Gamma(x, x_t)^\top]^\top$  is an  $nt \times n$  matrix. Notice that  $G_t(x)$  can be interpreted as an embedding of a point  $x$  supported over the points  $x_1, \dots, x_t$  observed so far. Now, if an arm  $x$  is sufficiently unexplored, the estimate  $\mu_t(x)$  will, in general, have high variance. One natural way of specifying the uncertainty around  $\mu_t(x)$  is the following multi-task kernel:

$$\Gamma_t(x, x') = \Gamma(x, x') - G_t(x)^\top (G_t + \eta I_{nt})^{-1} G_t(x'), \quad x, x' \in \mathcal{X}. \quad (1)$$

To see this, we draw a connection to multi-task Gaussian processes (MT-GPs) (Liu et al., 2018). Let  $f \sim \mathcal{GP}(0, \Gamma)$  be a sample from a zero-mean MT-GP with covariance function  $\Gamma$  (i.e.,  $\mathbb{E}[f_i(x)] = 0$  and  $\mathbb{E}[f_i(x)f_j(x')] = \Gamma(x, x')_{ij}$  for all  $i, j \in [n]$  and  $x, x' \in \mathcal{X}$ ), and assume that the observation noise vectors  $\{\varepsilon_t\}_{t \geq 1}$  are independent and  $\mathcal{N}(0, \eta I_{nt})$  distributed. Then the posterior distribution of  $f$  conditioned on the data  $\{(x_i, y_i)\}_{i=1}^t$  is also a MT-GP with mean  $\mu_t$  and covariance  $\Gamma_t$ , yielding a natural uncertainty model. Now, inspired by the optimism-in-face-of-uncertainty principle, we compute the acquisition function for the next round as

$$u_{t+1}(x) = s_{\lambda_{t+1}}(\mu_t(x)) + L_{\lambda_{t+1}} \beta_t \|\Gamma_t(x, x)\|^{1/2}, \quad (2)$$

where  $L_\lambda$  is the Lipschitz constant of the scalarization  $s_\lambda$ . As a result, selecting the arm  $x_{t+1}$  with the highest  $u_{t+1}$  inherently trades off exploitation, i.e., picking points with high (scalarized) reward  $s_{\lambda_{t+1}}(\mu_t(x))$ , with exploration, i.e., picking points with high uncertainty  $\|\Gamma_t(x, x)\|^{1/2}$ . The parameter  $\beta_t$  balances between these two objectives, and needs to be tuned properly to guarantee low regret. The pseudo-code of MT-KB is given in Algorithm 1.

**Computational complexity** Maximizing the acquisition function  $u_t(x)$  over  $\mathcal{X}$  is in general NP-hard even for a single task, since it is a highly non-convex function. To simplify the exposition, in what follows, we will assume that an efficient oracle to optimize  $u_t(x)$ , such as DIRECT (Brochu et al., 2010), is provided to us, and the per step cost comes only from computing  $u_t(x)$ . Now, the cost of computing  $u_t(x)$  is dominated by the cost of inversion of the  $nt \times nt$  kernel matrix, and thus in principle scales as  $O(n^3 t^3)$ .<sup>4</sup> We note that the cubic dependency with time  $t$  is present even in the single-task ( $n = 1$ ) setting (Shahriari et al., 2015) and in this case, in fact, MT-KB reduces to the GP-UCB algorithm (Srinivas et al., 2010).

<sup>4</sup>This can be reduced to  $O(n^3 t^2)$  using Schur's complement, but at an additional storage cost of  $O(n^2 t^2)$ .

---

**Algorithm 1** Multi-task kernelized bandits (MT-KB)

---

**Require:** Kernel  $\Gamma$ , distribution  $P_\lambda$ , scalarization  $s_\lambda$ , time budget  $T$ , parameters  $\eta$ ,  $\{\beta_t\}_{t=0}^{T-1}$

Initialize  $\mu_0(x) = 0$  and  $\Gamma_0(x, x') = \Gamma(x, x')$

**for** round  $t = 1, 2, 3, \dots, T$  **do**

    Sample weight vector  $\lambda_t \sim P_\lambda$

    Compute acquisition function  $u_t(x) = s_{\lambda_t}(\mu_{t-1}(x)) + L_{\lambda_t} \beta_{t-1} \|\Gamma_{t-1}(x, x)\|^{1/2}$

    Select point  $x_t \in \operatorname{argmax}_{x \in \mathcal{X}} u_t(x)$

    Get vector-valued output  $y_t = f(x_t) + \varepsilon_t$

    Compute

$$G_t(x) = [\Gamma(x_1, x)^\top, \dots, \Gamma(x_t, x)^\top]^\top, \quad G_t = [\Gamma(x_i, x_j)]_{i,j=1}^t, \quad Y_t = [y_1^\top, \dots, y_t^\top]^\top$$

    Update

$$\begin{aligned} \mu_t(x) &= G_t(x)^\top (G_t + \eta I_{nt})^{-1} Y_t \\ \Gamma_t(x, x) &= \Gamma(x, x) - G_t(x)^\top (G_t + \eta I_{nt})^{-1} G_t(x) \end{aligned}$$

**end for**

---

**Remark 1** The diagonal MT kernel  $\Gamma(x, x') = \operatorname{diag}(k_1(x, x'), \dots, k_n(x, x'))$  corresponds to treating each task independently and the problem reduces to inverting  $n$  kernel matrices yielding a per-step cost of  $O(nt^3)$  for MT-KB. This is similar to the prior works (Hernández-Lobato et al., 2016; Paria et al., 2019; Belakaria et al., 2019) which assume that each task  $f_i$  is sampled independently from the scalar Gaussian process  $\mathcal{GP}(0, k_i)$ .

One common approach to improve computational scalability in kernel methods is the Nyström approximation (Drineas and Mahoney, 2005), which restricts the embeddings  $G_t(x)$  and the kernel matrix  $G_t$  to be supported on a subset (dictionary)  $\mathcal{D}_t$  of selected points. However, this can lead to sub-optimal choices and large regret if  $\mathcal{D}_t$  is not sufficiently accurate. This brings about a trade-off between larger and more accurate dictionaries, or smaller and more efficient ones. The BKB algorithm solves this for single-task BO (Calandriello et al., 2019). We now generalize BKB for multiple tasks to improve over the  $O(n^3 t^3)$  cost of MT-KB.

### 3.2 Algorithm 2: Multi-task budgeted kernelized bandits (MT-BKB)

The central idea behind this algorithm is to evaluate an approximate acquisition function  $\tilde{u}_t(x)$ , which remains a valid UCB over the scalarized function  $s_{\lambda_t}(f(x))$  and at the same time is sufficiently close to  $u_t(x)$  to ensure low regret. Given the data  $\{(x_i, y_i)\}_{i=1}^t$ , we start with an empty dictionary  $\mathcal{D}_t = \emptyset$  and iterate over the set  $\{x_1, \dots, x_t\}$  to update  $\mathcal{D}_t$  as follows. For each candidate  $x_i$ , we compute an inclusion probability  $p_{t,i}$ , and add  $x_i$  to  $\mathcal{D}_t$  with probability  $p_{t,i}$ . The inclusion probabilities  $p_{t,i}$  need to be set suitably so that the dictionary is small enough without compromising on



its accuracy. Once the sampling is over, let  $\mathcal{D}_t$  be given by the set  $\{x_{i_1}, \dots, x_{i_{m_t}}\}$ , where  $m_t$  is the size of  $\mathcal{D}_t$  and  $i_j \in [t]$  for each  $j \in [m_t]$ . Given the dictionary  $\mathcal{D}_t$ , let  $\tilde{G}_t(x) = [\Gamma(x_{i_1}, x)^\top / \sqrt{p_{t,i_1}}, \dots, \Gamma(x_{i_{m_t}}, x)^\top / \sqrt{p_{t,i_{m_t}}}]^\top$  be the  $nm_t \times n$  embedding of  $x$  supported over all points in  $\mathcal{D}_t$  and  $\tilde{G}_t = [\Gamma(x_{i_u}, x_{i_v}) / \sqrt{p_{t,i_u} p_{t,i_v}}]_{u,v=1}^{m_t}$  be the corresponding  $nm_t \times nm_t$  kernel matrix, properly reweighted by the inclusion probabilities. Then we compute the Nyström embeddings as

$$\tilde{\Phi}_t(x) = (\tilde{G}_t^{1/2})^+ \tilde{G}_t(x),$$

where  $(\cdot)^+$  denotes the pseudo-inverse. We now use these embeddings to approximate  $\mu_t$  and  $\Gamma_t$  as

$$\tilde{\mu}_t(x) = \tilde{\Phi}_t(x)^\top (\tilde{V}_t + \eta I_{nm_t})^{-1} \sum_{s=1}^t \tilde{\Phi}_t(x_s) y_s,$$

$$\tilde{\Gamma}_t(x, x') = \Gamma(x, x') - \tilde{\Phi}_t(x)^\top \tilde{\Phi}_t(x') + \eta \tilde{\Phi}_t(x)^\top (\tilde{V}_t + \eta I_{nm_t})^{-1} \tilde{\Phi}_t(x'),$$

where  $\tilde{V}_t = \sum_{s=1}^t \tilde{\Phi}_t(x_s) \tilde{\Phi}_t(x_s)^\top$  is an  $nm_t \times nm_t$  matrix. Finally, similar to (2), we compute the acquisition function for the next round as

$$\tilde{u}_{t+1}(x) = s_{\lambda_{t+1}}(\tilde{\mu}_t(x)) + L_{\lambda_{t+1}} \tilde{\beta}_t \|\tilde{\Gamma}_t(x, x)\|^{1/2},$$

with  $\tilde{\beta}_t$  governing the exploration-exploitation tradeoff. The inclusion probabilities for the next round are computed as  $p_{t+1,i} = \min\{q \|\tilde{\Gamma}_t(x_i, x_i)\|, 1\}$ , where  $q \geq 1$  is a parameter trading-off the size of the dictionary and accuracy of the approximation. We note here that constructing  $\mathcal{D}_t$  based on approximate posterior variance sampling is well-studied for scalar kernels (Alaoui and Mahoney, 2015), and in this work, we introduce it for the first time for MT kernels. The pseudo-code of MT-BKB is given in Algorithm 2.

**Computational complexity** Computing the dictionary involves a linear search over all selected points while the inclusion probabilities are computed already at the previous round, and thus requires  $O(t)$  time per step. The Nyström embeddings  $\tilde{\Phi}_t(x)$  can be computed in  $O(n^3 m_t^3)$  time, since an inversion of the matrix  $\tilde{G}_t$  is required. By using these embeddings,  $\tilde{V}_t$  can now be computed and inverted in  $O(n^2 m_t^2 t)$  and  $O(n^3 m_t^3)$  time, respectively. Since, in general,  $m_t \leq t$ , the total per step cost of computing the acquisition function  $\tilde{u}_t(x)$  is now  $O(n^3 m_t^2 t)$  as opposed to the  $O(n^3 t^3)$  cost of MT-KB. The computational advantage of MT-BKB is clearly visible when the dictionary size  $m_t$  is near constant at every step, i.e., when  $m_t = \tilde{O}(1)$ , where  $\tilde{O}(\cdot)$  hides constant and log factors. We shall see in Section 4.1 that this holds, for example, for the intrinsic coregionalization model (ICM) with the squared exponential kernel in its scalar part.

### 3.3 Improved computational complexity for ICM kernels

The computational cost of our algorithms can be greatly reduced for ICM kernels  $\Gamma(x, x') = k(x, x')B$ . Let  $\{\xi_i\}_{i=1}^n$  be the eigenvalues of  $B$  with corresponding orthonormal eigenvectors  $\{u_i\}_{i=1}^n$ . We then have the kernel matrix  $G_t = \sum_{i=1}^n \xi_i K_t \otimes u_i u_i^\top$  and

---

**Algorithm 2** Multi-task budgeted kernelized bandits (MT-BKB)

---

**Require:** Kernel  $\Gamma$ , distribution  $P_\lambda$ , scalarization  $s_\lambda$ , time budget  $T$ , parameters  $\eta, q, \{\tilde{\beta}_t\}_{t=0}^{T-1}$

Initialize  $\tilde{\mu}_0(x) = 0$  and  $\tilde{\Gamma}_0(x, x') = \Gamma(x, x')$

**for** round  $t = 1, 2, 3, \dots, T$  **do**

    Sample weight vector  $\lambda_t \sim P_\lambda$

    Compute acquisition function  $\tilde{u}_t(x) = s_{\lambda_t}(\tilde{\mu}_{t-1}(x)) + L_{\lambda_t} \tilde{\beta}_{t-1} \|\tilde{\Gamma}_{t-1}(x, x)\|^{1/2}$

    Select point  $x_t \in \operatorname{argmax}_{x \in \mathcal{X}} \tilde{u}_t(x)$

    Get vector-valued output  $y_t = f(x_t) + \varepsilon_t$

    Initialize dictionary  $\mathcal{D}_t = \emptyset$

**for**  $i = 1, 2, 3, \dots, t$  **do**

        Set inclusion probability  $p_{t,i} = \min \left\{ q \|\tilde{\Gamma}_{t-1}(x_i, x_i)\|, 1 \right\}$

        Draw  $z_{t,i} \sim \text{Bernoulli}(p_{t,i})$

**if**  $z_{t,i} = 1$  **then**

            Update  $\mathcal{D}_t = \mathcal{D}_t \cup \{x_i\}$

**end if**

**end for**

    Set  $m_t = |\mathcal{D}_t|$ , enumerate  $\mathcal{D}_t = \{x_{i_1}, \dots, x_{i_{m_t}}\}$  and compute

$$\tilde{G}_t(x) = \left[ \frac{1}{\sqrt{p_{t,i_1}}} \Gamma(x_{i_1}, x)^\top, \dots, \frac{1}{\sqrt{p_{t,i_{m_t}}}} \Gamma(x_{i_{m_t}}, x)^\top \right]^\top, \quad \tilde{G}_t = \left[ \frac{1}{\sqrt{p_{t,i_u} p_{t,i_v}}} \Gamma(x_{i_u}, x_{i_v}) \right]_{u,v=1}^{m_t}$$

    Find Nyström embeddings  $\tilde{\Phi}_t(x) = \left( \tilde{G}_t^{1/2} \right)^+ \tilde{G}_t(x)$

    Compute  $\tilde{V}_t = \sum_{s=1}^t \tilde{\Phi}_t(x_s) \tilde{\Phi}_t(x_s)^\top$  and update

$$\begin{aligned} \tilde{\mu}_t(x) &= \tilde{\Phi}_t(x)^\top (\tilde{V}_t + \eta I_{nm_t})^{-1} \sum_{s=1}^t \tilde{\Phi}_t(x_s) y_s \\ \tilde{\Gamma}_t(x, x) &= \Gamma(x, x) - \tilde{\Phi}_t(x)^\top \tilde{\Phi}_t(x) + \eta \tilde{\Phi}_t(x)^\top (\tilde{V}_t + \eta I_{nm_t})^{-1} \tilde{\Phi}_t(x) \end{aligned}$$

**end for**

---

the output vector  $Y_t = \sum_{i=1}^n Y_t^i \otimes u_i$ , where  $\otimes$  denotes the Kronecker product,  $K_t = [k(x_i, x_j)]_{i,j=1}^t$  is the kernel matrix of the scalar kernel  $k$  and  $Y_t^i = [y_1^\top u_i, \dots, y_t^\top u_i]^\top$ . Plugging these into (3.1) and (1), and using properties of Kronecker product, we now obtain

$$\begin{aligned} \mu_t(x) &= \sum_{i=1}^n \xi_i k_t(x)^\top (\xi_i K_t + \eta I_t)^{-1} Y_t^i u_i, \\ \|\Gamma_t(x, x)\| &= \max_{1 \leq i \leq n} \xi_i \left( k(x, x) - \xi_i k_t(x)^\top (\xi_i K_t + \eta I_t)^{-1} k_t(x) \right), \end{aligned}$$

where  $k_t(x) = [k(x_1, x), \dots, k(x_t, x)]^\top$ . We see that the eigen-decomposition of  $B$  needs to be computed only once at the beginning and then, in the new coordinate system, we essentially have to solve  $n$  independent problems. Specifically, at round  $t$ , we

need to project the vector-valued output  $y_t$  to all coordinates and compute  $n$  matrix-vector multiplications of size  $t$ . However, since the kernel matrix  $K_t$  is rescaled by the eigenvalues  $\xi_i$ , we have to perform only one  $t \times t$  inversion. Hence, the per-step time complexity of MT-KB is now  $O(n^2 + (n+t)t^2)$  as opposed to  $O(n^3t^3)$  for general MT kernels. Similarly, the per-step cost of MT-BKB can be substantially improved to  $O(n^2 + (n+m_t)m_t t)$  from the  $O(n^3m_t^2t)$  cost in general. Therefore, the kernels of this form allow for a near-linear (in time  $t$ ) per-step cost of MT-BKB at the price of the eigen-decomposition of  $B$ . (We defer the details to appendix A.)

## 4 Theoretical results

We now present the first theoretical result of this work, a concentration inequality for the estimate of the unknown multi-task objective function  $f$ , which is then used to prove the regret bounds for our algorithms. (Complete proofs of all results presented in this section are deferred to the appendix.)

**Theorem 1 (Multi-task concentration inequality)** *Let  $f \in \mathcal{H}_\Gamma(\mathcal{X})$  and the noise vectors  $\{\varepsilon_t\}_{t \geq 1}$  be  $\sigma$ -sub-Gaussian. Then, for any  $\eta > 0$  and  $\delta \in (0, 1]$ , with probability at least  $1 - \delta$ , the following holds uniformly over all  $x \in \mathcal{X}$  and  $t \geq 1$ :*

$$\|f(x) - \mu_t(x)\|_2 \leq \left( \|f\|_\Gamma + \frac{\sigma}{\sqrt{n}} \sqrt{2 \log(1/\delta) + \log \det(I_{nt} + \eta^{-1} G_t)} \right) \|\Gamma_t(x, x)\|^{1/2}.$$

The significance of this bound can be better understood by studying the log-determinant term, and for this, we again draw a connection to MT-GPs. If  $f \sim \mathcal{GP}(0, \Gamma)$  and  $\varepsilon_t \sim \mathcal{N}(0, \eta I_n)$  i.i.d., then the *mutual information* between  $f$  and the outputs  $Y_t$  is exactly equal to  $\frac{1}{2} \log \det(I_{nt} + \eta^{-1} G_t)$ , and it is a measure for the reduction in the uncertainty or, equivalently, the information gain about  $f$ . Note that while we use GPs to describe the uncertainty in estimating the unknown function  $f$ , the bound is *frequentist* and does not need any *Bayesian* assumption about  $f$ . Similar to the single-task setting (Durand et al., 2018), the bound is proved by deriving a new self-normalized concentration inequality for martingales in the  $\ell_2$  space.<sup>5</sup> We note here that Astudillo and Frazier (2019) consider the much simpler setting of noise-free outputs and their bound can be re-derived as a special case of Theorem 1.

**Remark 2** *The multi-task kernel  $\Gamma$  can be seen as a scalar kernel,  $\Gamma(x, x')_{ij} = k((x, i), (x', j))$ ,  $i, j \in [n]$ , and  $G_t$  as an  $nt \times nt$  kernel matrix of  $k$  evaluated at points  $(x_s, i)$ ,  $s \in [t]$ ,  $i \in [n]$ . In this case, one can use Chowdhury and Gopalan (2017, Theorem 2) to derive concentration bounds for each task  $f_i$  separately and combine them together to obtain a result similar to Theorem 1 but with a notable change –  $\|\Gamma_t(x, x)\|$  being replaced by  $\text{trace}(\Gamma_t(x, x))$ . Thus, in general, we prove a tighter concentration inequality which eventually leads to a  $O(\sqrt{n})$  factor saving in the final regret bound.*

<sup>5</sup>Theorem 1 can even be generalized to the regime of infinite-task learning (Kadri et al., 2016; Brault et al., 2019), where the observations lie in a Hilbert space  $\mathcal{H}$ , and thus can be of independent interest. The only technical assumption that one will need is that the multi-task kernel  $\Gamma(x, x)$  has a finite trace, which trivially holds in the finite-task setting.

## 4.1 Regret bounds

Theorem 1 allows for a principled way to tune the confidence radii (i.e.,  $\beta_t$  and  $\tilde{\beta}_t$ ) of our algorithms and achieve low regret. We now present the regret bound of MT-KB, which, to the best of our knowledge, is the first frequentist regret guarantee for multi-task BO under any general MT kernel.

**Theorem 2 (Cumulative regret of MT-KB)** *Let  $f \in \mathcal{H}_\Gamma(\mathcal{X})$ ,  $\|f\|_\Gamma \leq b$  and  $\|\Gamma(x, x)\| \leq \kappa$  for all  $x \in \mathcal{X}$ . Let the scalarization function  $s_\lambda$  be  $L_\lambda$ -Lipschitz,  $L_\lambda \leq L$  for all  $\lambda \in \Lambda$  and the noise vectors  $\{\varepsilon_t\}_{t \geq 1}$  be  $\sigma$ -sub-Gaussian. Then, for any  $\eta > 0$  and  $\delta \in (0, 1]$ , MT-KB with*

$$\beta_t = b + \frac{\sigma}{\sqrt{\eta}} \sqrt{2 \log(1/\delta) + \sum_{s=1}^t \log \det (I_n + \eta^{-1} \Gamma_{s-1}(x_s, x_s))},$$

*enjoys, with probability at least  $1 - \delta$ , the regret bound*

$$R_C^{MT-KB}(T) \leq 2L \left( b + \frac{\sigma}{\sqrt{\eta}} \sqrt{(2 \log(1/\delta) + \gamma_{nT}(\Gamma, \eta))} \right) \sqrt{(1 + \kappa/\eta) T \sum_{t=1}^T \|\Gamma_t(x_t, x_t)\|},$$

*where  $\gamma_{nT}(\Gamma, \eta) := \max_{\mathcal{X}_T \subset \mathcal{X}} \frac{1}{2} \log \det (I_{nT} + \eta^{-1} G_T)$  denotes the maximum information gain.*

Theorem 2, along with the upper bound  $\sum_{t=1}^T \|\Gamma_t(x_t, x_t)\| \leq 2\eta\gamma_{nT}(\Gamma, \eta)$ , yields the more compact regret bound  $\tilde{O}(b\sqrt{T\gamma_{nT}(\Gamma, \eta)} + \gamma_{nT}(\Gamma, \eta)\sqrt{T})$ . We note here that the bound for single-task case (Chowdhury and Gopalan, 2017) can be recovered by setting  $n = 1$ . Furthermore, since the single-task bound is shown to be tight upto a poly-logarithmic factor (Scarlett et al., 2017), our bound, we believe, is also tight in terms of dependence on  $T$ . Now, we instantiate Theorem 2 for the special case of separable kernels to point out the novel insights and improvements that our analysis unearths as compared to existing work.

**Lemma 1 (Inter-task structure in regret bound)** *Let  $B$  be an  $n \times n$  p.s.d. matrix and  $\Gamma(x, x') = k(x, x')B$ . Let  $\|\Gamma(x, x)\| \leq \kappa$  and  $k(x, x) = 1$  for all  $x \in \mathcal{X}$ . Then the following holds:*

$$\begin{aligned} \gamma_{nT}(\Gamma, \eta) &\leq \sum_{i \in [n]: \xi_i > 0} \gamma_T(k, \eta/\xi_i), \\ \sum_{t=1}^T \|\Gamma_t(x_t, x_t)\| &\leq 2\eta \max\{\kappa, 1\} \gamma_T(k, \eta), \end{aligned}$$

*where  $\xi_1, \dots, \xi_n$  are the eigenvalues of  $B$  and  $\gamma_T(k, \alpha) := \max_{\mathcal{X}_T \subset \mathcal{X}} \frac{1}{2} \log \det (I_T + \alpha^{-1} K_T)$ ,  $\alpha > 0$ , is the maximum information gain associated with the scalar kernel  $k$ .*

Lemma 1, along with Theorem 2, leads to a regret bound that explicitly encodes the amount of similarity between tasks in terms of the spectral properties of  $B$ . For

example, consider the case  $B = \omega I_n + (1 - \omega)1_n/n$ ,  $\omega \in [0, 1]$ , which has one eigenvalue equal to 1 and all others equal to  $\omega$ . In this case, we obtain  $\gamma_{nT}(\Gamma, \eta) \leq \gamma_T(k, \eta) + (n - 1)\gamma_T(k, \eta/\omega)$ . Now  $\gamma_T(k, \eta/\omega)$  is an increasing function in  $\omega$ , and in fact,  $\gamma_T(k, \eta/\omega) = 0$  when  $\omega = 0$ . Hence, a low value of  $\omega$ , i.e., a high amount of similarity between tasks, yields a low cumulative regret and vice-versa. (A numerical example is shown in Figure 1: (a) using the squared exponential kernel as  $k$ .) Moreover, for the extreme two cases of  $\omega = 0$  (all tasks identical) and  $\omega = 1$  (all tasks unrelated), the regret bounds are  $\tilde{O}(\gamma_T(k, \eta)\sqrt{T})$  and  $\tilde{O}(\gamma_T(k, \eta)\sqrt{nT})$ , respectively. The bounds clearly assert that similar objectives can be learnt much faster together rather than learning them separately. To the best of our knowledge, this intuitive but important observation is not captured by any of the existing regret analysis (Zuluaga et al., 2013; Paria et al., 2019; Belakaria et al., 2019).

**Remark 3** Existing works model each task independently by means of a diagonal multi-task kernel  $\Gamma(x, x') = \text{diag}(k_1(x, x'), \dots, k_n(x, x'))$  and prove regret bounds for this special setting. In contrast, Theorem 2 is applicable to any general multi-task kernel, and in the special case of diagonal kernel, yields, along with Lemma 1, a regret bound of  $\tilde{O}(\max_i \gamma_T(k_i, \eta)\sqrt{nT})$ . This bound, together with the discussion above, suggest that whereas on the one hand MT-KB exploits similarities between tasks efficiently, its performance on the other hand does not suffer when the tasks are unrelated. Another important point to note here is that we analyze the frequentist (worst-case) regret, which is a stronger notion of regret compared to the Bayesian one (defined as the expected cumulative regret under a prior distribution of  $f$ ) as considered in previous works (Paria et al., 2019; Belakaria et al., 2019).

We now present regret and complexity guarantees for MT-BKB, which, to the best of our knowledge, are first of their kinds for multi-task BO under kernel or GP approximation.

**Theorem 3 (Analysis of MT-BKB)** For any  $\eta > 0$ ,  $\varepsilon \in (0, 1)$  and  $\delta \in (0, 1]$ , let  $\rho = (1 + \varepsilon)/(1 - \varepsilon)$  and  $q = 6\rho \log(4T/\delta)/\varepsilon^2$ . Then, under the same hypothesis as Theorem 2, if we run MT-BKB with

$$\tilde{\beta}_t = b(1 + 1/\sqrt{1 - \varepsilon}) + \frac{\sigma}{\sqrt{\eta}} \sqrt{2 \log(2/\delta) + \rho \sum_{s=1}^t \log \det(I_n + \eta^{-1} \tilde{\Gamma}_{s-1}(x_s, x_s))},$$

then, with probability at least  $1 - \delta$ , the following holds:

$$\begin{aligned} R_C^{MT-BKB}(T) &\leq 2\rho^{3/2} R_C^{MT-KB}(T), \\ \forall t \in [T], \quad m_t &\leq 6\rho q(1 + \kappa/\eta) \sum_{s=1}^t \|\Gamma_s(x_s, x_s)\|. \end{aligned}$$

Theorem 3 shows that MT-BKB can achieve an order-wise similar regret scaling as MT-KB (up to a constant factor), but only at a fraction of the computational cost. To see this, we again consider the kernel  $\Gamma(x, x') = k(x, x')B$ . In this case, Theorem 3 and Lemma 1 together imply that the dictionary size  $m_t$  is  $\tilde{O}(\gamma_t(k, \eta))$ . Now  $\gamma_t$  is itself

bounded for specific scalar kernels  $k$ , e.g., it is  $O((\ln t)^d)$  for the squared exponential kernel (Srinivas et al., 2010), yielding  $m_t$  to be  $\tilde{O}(1)$ . This leads to a near-linear (in time  $t$ ) per-step cost for MT-BKB compared to the cubic cost for MT-KB. Further, it is worth noting that MT-BKB can adapt to any desired accuracy level  $\varepsilon$  of the Nyström approximation. A low value of  $\varepsilon$  corresponds to high desired accuracy and MT-BKB adapts to it by inducing more and more points in the dictionary, yielding accurate embeddings and thus, in turn, low regret. Conversely, if one is willing to compromise on the accuracy (given by a high value of  $\varepsilon$ ), then MT-BKB can greatly reduce the size of the dictionary, yielding a low time complexity. The analysis follows in the footsteps of Calandriello et al. (2019), but is carefully generalized to consider multi-task kernels. The regret bound is crucially achieved by showing that  $\Gamma_t(x, x)/\rho \preceq \tilde{\Gamma}_t(x, x) \preceq \rho\Gamma_t(x, x)$ , i.e., MT-BKB’s variance estimates are always almost close to the exact ones ( $A \succeq B$  denotes that the matrix  $A - B$  is p.s.d.). This not only helps us avoid variance starvation which is known to happen with classical sparse GP approximations (Wang et al., 2018), but also, allows us to set  $\tilde{\beta}_t$  efficiently and in a data-adaptive way.

## 5 Experiments

In order to investigate the practical benefits offered by learning with multi-task kernels, we compare MT-KB and MT-BKB with single-task algorithms that enjoy regret guarantees under RKHS smoothness assumptions. Specifically, we consider GP-UCB (Chowdhury and Gopalan, 2017) and its Nyström approximation BKB (Calandriello et al., 2019) as baselines, where each task is learnt independently and inter-task structure is not exploited. We call these baselines *independent task kernelized bandits (IT-KB)* and *budgeted kernelized bandits (IT-BKB)*, respectively. Whenever the objective is not explicitly generated from an RKHS, we also compare with MOBO (Paria et al., 2019), which has better regret performance than other methods (Knowles, 2006; Ponweiser et al., 2008; Emmerich and Klinkenberg, 2008; Hernández-Lobato et al., 2016) that model each task with an independent GP. In all simulations, we set  $\eta = 0.1$ ,  $\delta = 0.1$  and  $\varepsilon = 0.5$ , and use the Chebyshev scalarization. Similar to (Paria et al., 2019), we sample from  $P_\lambda$  as  $\lambda = \alpha/\|\alpha\|_1$ , where  $\alpha_i = \|u\|_1/u_i$ ,  $i \in [n]$ , and  $u$  is sampled uniformly from  $[0, 1]^n$ . We compare the algorithms on the following MOO problems and plot mean and standard deviation (over 10 independent trials) of the time-average cumulative regret  $\frac{1}{T}R_C(T)$  in Fig. 1: (b)-(f). (More details in appendix E.)

**RKHS function** We generate a vector-valued RKHS element as  $f(\cdot) = \sum_{i \leq 50} \Gamma(\cdot, x_i)c_i$ , where the domain  $\mathcal{X}$  is an 0.01-net of the interval  $[0, 1]$ , each  $x_i \in \mathcal{X}$  and each  $c_i$  is uniformly sampled from  $[-1, 1]^n$ . We consider the ICM kernel  $\Gamma(x, x') = k(x, x')B$  adopting a SE kernel with lengthscale 0.2 for its scalar part and set  $B = A^\top A$ , where the elements of the  $n \times n$  matrix  $A$  is uniformly sampled from  $[0, 1]$ . We set  $\kappa$  as the largest eigenvalue of  $B$  and bound the RKHS norm of  $f$  using  $b = \max_x \|f(x)\|_2/\kappa$ . The noise vectors are taken i.i.d.  $\mathcal{N}(0, \sigma^2 I_n)$ ,  $\sigma = 0.1$ . We compare the algorithms for  $n = 2$  and  $n = 20$  tasks. We observe that learning with MT kernels is much faster than learning the tasks independently – even more so when no. of tasks are higher (Fig. 1: (b), (c)).

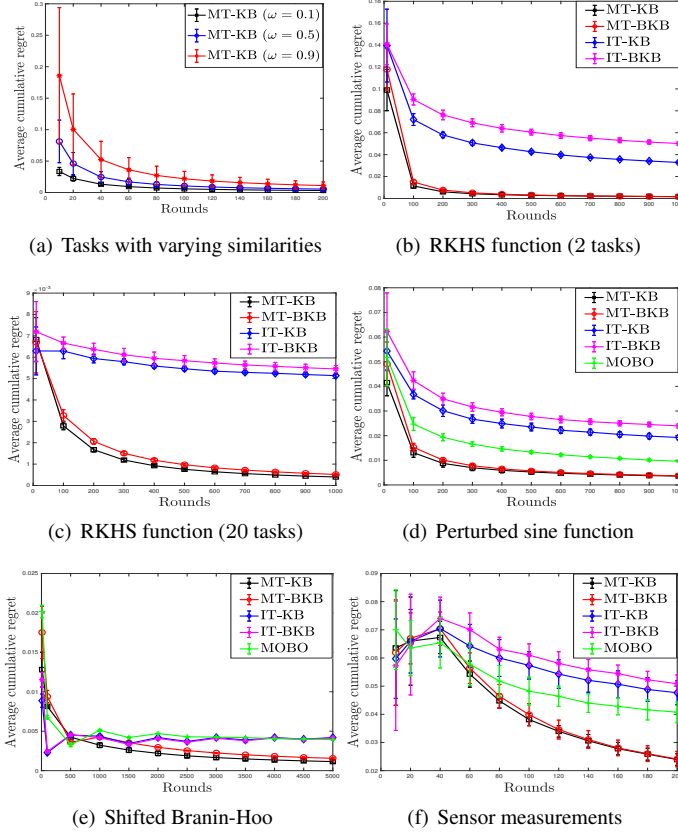


Figure 1: (a) Regret performance of MT-KB under varying inter-task similarities, (b)-(f) Comparison of average cumulative regret of MT-KB and MT-BKB with IT-KB, IT-BKB and MOBO on different MOO problems.

**Perturbed sine function** We study a setting similar to (Baldassarre et al., 2012), where  $\mathcal{X}$  is an 0.01-net of the interval  $[0, 1]$  and we have  $n = 4$  tasks. Each task is given by a function  $f_i(x) = \sin(2\pi x) + 0.6f_i^{\text{pert}}(x)$  corrupted by Gaussian noise of variance 0.01. Each perturbation function  $f_i^{\text{pert}}$  is a weighted sum of three Gaussians of width 0.1 centered at  $x_1 = 0.05$ ,  $x_2 = 0.4$  and  $x_3 = 0.7$ , where task-specific weights are carefully chosen in order to yield tasks that are related by the common function, but also have local differences. We use the kernel  $\Gamma_\omega(x, x') = k(x, x')(\omega I_n + (1 - \omega)1_n/n)$  that imposes a common similarity among all components and results are shown for  $\omega = 0.4$  (Fig. 1: (d)).

**Shifted Branin-Hoo** The Branin-Hoo function, defined over a subset of  $\mathbb{R}^2$ , is a common benchmark for BO (Jones, 2001). We consider 9 shifted Branin-Hoo's as related tasks, where the  $i$ -th task is a translation of the function by  $i\%$  along either axis,

and run algorithms with the kernel  $\Gamma_\omega$ ,  $\omega = 0.5$  (Fig. 1: (e)).

**Sensor measurements** We take temperature, light and humidity measurements from 54 sensors collected in the Intel Berkeley lab (Srinivas et al., 2010) in the context of MOO. We have 3 tasks, one for each variable, and each task  $f_i(x)$  is given by the empirical mean of 50% of the readings recorded at the sensor placed at location  $x$ . We take remaining readings to estimate an ICM kernel and run our algorithms with this kernel. Specifically, for its scalar part, we fit an SE kernel on sensor locations, and for its matrix part, we estimate inter-task similarities as  $B = \frac{1}{m} R^\top K^{-1} R$ , where  $m$  denotes number of readings,  $R$  is an  $m \times 3$  matrix of readings for all tasks and  $K$  is the  $m \times m$  gram matrix of SE kernel. The idea is to de-correlate  $R$  with  $K^{-1}$  first so that only correlation with respect to  $B$  is left. Further, we compute the empirical variance of sensor readings for each task and take the largest of those as  $\sigma^2$ . We see that the regret performance of MT-KB and MT-BKB are much better than IT-KB, IT-BKB and MOBO that do not use the inter-task structure in the form of the matrix  $B$  (Fig. 1: (f)).

## 6 Concluding remarks

To the best of our knowledge, we prove the first rigorous regret bounds for multi-task Bayesian optimization that capture inter-task dependencies. We have demonstrated the shortcoming of modelling each task independently without making use of task similarities, and developed algorithms using multi-task kernels, which perform well in practice. We believe that our regret bounds are tight in terms of dependence on the time horizon. However, whether the dependence on the inter-task structure is optimal or not remains an important open question. It would also be interesting to see whether our multi-task concentration can be applied to several other interesting settings, for example optimizing under heavy-tailed corruptions (Chowdhury and Gopalan, 2019a), with a batch of inputs (Desautels et al., 2014), learning with kernel mean embeddings (Chowdhury et al., 2020), modelling the transition structure of a Markov decision process (Chowdhury and Gopalan, 2019b) to name a few.

## References

- Ahmed Alaoui and Michael W Mahoney. Fast randomized kernel ridge regression with statistical guarantees. In *Advances in Neural Information Processing Systems*, pages 775–783, 2015.
- Mauricio A Alvarez, Lorenzo Rosasco, and Neil D Lawrence. Kernels for vector-valued functions: A review. *arXiv preprint arXiv:1106.6251*, 2011.
- Raul Astudillo and Peter Frazier. Bayesian optimization of composite functions. In *International Conference on Machine Learning*, pages 354–363, 2019.
- Luca Baldassarre, Lorenzo Rosasco, Annalisa Barla, and Alessandro Verri. Multi-output learning via spectral filtering. *Machine learning*, 87(3):259–301, 2012.



- Syrine Belakaria, Aryan Deshwal, and Janardhan Rao Doppa. Max-value entropy search for multi-objective bayesian optimization. In *Advances in Neural Information Processing Systems*, pages 7823–7833, 2019.
- Edwin V Bonilla, Kian M Chai, and Christopher Williams. Multi-task gaussian process prediction. In *Advances in neural information processing systems*, pages 153–160, 2008.
- Romain Brault, Alex Lambert, Zoltan Szabo, Maxime Sangnier, and Florence d’Alche Buc. Infinite task learning in rkhs. In *The 22nd International Conference on Artificial Intelligence and Statistics*, pages 1294–1302, 2019.
- Eric Brochu, Vlad M Cora, and Nando De Freitas. A tutorial on bayesian optimization of expensive cost functions, with application to active user modeling and hierarchical reinforcement learning. *arXiv preprint arXiv:1012.2599*, 2010.
- Daniele Calandriello, Luigi Carratino, Alessandro Lazaric, Michal Valko, and Lorenzo Rosasco. Gaussian process optimization with adaptive sketching: Scalable and no regret. In *Conference on Learning Theory*, 2019.
- Andrea Caponnetto, Charles A Micchelli, Massimiliano Pontil, and Yiming Ying. Universal multi-task kernels. *Journal of Machine Learning Research*, 9(Jul):1615–1646, 2008.
- Claudio Carmeli, Ernesto De Vito, Alessandro Toigo, and Veronica Umanit . Vector valued reproducing kernel hilbert spaces and universality. *Analysis and Applications*, 8(01):19–61, 2010.
- Rich Caruana. Multitask learning. *Machine learning*, 28(1):41–75, 1997.
- S. R. Chowdhury, Rafael dos Santos de Oliveira, and F. Ramos. Active learning of conditional mean embeddings via bayesian optimisation. 2020.
- Sayak Ray Chowdhury and Aditya Gopalan. On kernelized multi-armed bandits. In *Proceedings of the 34th International Conference on Machine Learning-Volume 70*, pages 844–853. JMLR. org, 2017.
- Sayak Ray Chowdhury and Aditya Gopalan. Bayesian optimization under heavy-tailed payoffs. In *Advances in Neural Information Processing Systems*, pages 13790–13801, 2019a.
- Sayak Ray Chowdhury and Aditya Gopalan. Online learning in kernelized markov decision processes. In *The 22nd International Conference on Artificial Intelligence and Statistics*, pages 3197–3205, 2019b.
- Thomas Desautels, Andreas Krause, and Joel W Burdick. Parallelizing exploration-exploitation tradeoffs in gaussian process bandit optimization. *Journal of Machine Learning Research*, 15:3873–3923, 2014.

- Petros Drineas and Michael W Mahoney. On the nyström method for approximating a gram matrix for improved kernel-based learning. *journal of machine learning research*, 6(Dec):2153–2175, 2005.
- Madalina M Drugan and Ann Nowe. Designing multi-objective multi-armed bandits algorithms: A study. In *The 2013 International Joint Conference on Neural Networks (IJCNN)*, pages 1–8. IEEE, 2013.
- Madalina M Drugan and Ann Nowé. Scalarization based pareto optimal set of arms identification algorithms. In *2014 International Joint Conference on Neural Networks (IJCNN)*, pages 2690–2697. IEEE, 2014.
- Audrey Durand, Odalric-Ambrym Maillard, and Joelle Pineau. Streaming kernel regression with provably adaptive mean, variance, and regularization. *The Journal of Machine Learning Research*, 19(1):650–683, 2018.
- Michael Emmerich and Jan-willem Klinkenberg. The computation of the expected improvement in dominated hypervolume of pareto front approximations. *Rapport technique, Leiden University*, 34:7–3, 2008.
- Theodoros Evgeniou, Charles A Micchelli, and Massimiliano Pontil. Learning multiple tasks with kernel methods. *Journal of machine learning research*, 6(Apr):615–637, 2005.
- R. Garnett, M. A. Osborne, and S. J. Roberts. Bayesian optimization for sensor set selection. In *Proceedings of the 9th ACM/IEEE International Conference on Information Processing in Sensor Networks, IPSN ’10*, pages 209–219, New York, NY, USA, 2010. ACM.
- Javier Gonzalez, Joseph Longworth, David C James, and Neil D Lawrence. Bayesian optimization for synthetic gene design. *arXiv preprint arXiv:1505.01627*, 2015.
- William H Greene. *Econometric analysis*. Pearson Education India, 2003.
- Steffen Grünewälder, Guy Lever, Luca Baldassarre, Sam Patterson, Arthur Gretton, and Massimiliano Pontil. Conditional mean embeddings as regressors. In *Proceedings of the 29th International Conference on Machine Learning*, pages 1803–1810, 2012.
- Chuan Guo, Geoff Pleiss, Yu Sun, and Kilian Q Weinberger. On calibration of modern neural networks. In *Proceedings of the 34th International Conference on Machine Learning-Volume 70*, pages 1321–1330. JMLR. org, 2017.
- Daniel Hernández-Lobato, Jose Hernandez-Lobato, Amar Shah, and Ryan Adams. Predictive entropy search for multi-objective bayesian optimization. In *International Conference on Machine Learning*, pages 1492–1501, 2016.
- Donald R Jones. A taxonomy of global optimization methods based on response surfaces. *Journal of global optimization*, 21(4):345–383, 2001.

- Hachem Kadri, Emmanuel Duflos, Philippe Preux, Stéphane Canu, Alain Rakotomamonjy, and Julien Audiffren. Operator-valued kernels for learning from functional response data. *The Journal of Machine Learning Research*, 17(1):613–666, 2016.
- Joshua Knowles. Parego: a hybrid algorithm with on-line landscape approximation for expensive multiobjective optimization problems. *IEEE Transactions on Evolutionary Computation*, 10(1):50–66, 2006.
- Haitao Liu, Jianfei Cai, and Yew-Soon Ong. Remarks on multi-output gaussian process regression. *Knowledge-Based Systems*, 144:102–121, 2018.
- Charles A Micchelli and Massimiliano Pontil. On learning vector-valued functions. *Neural computation*, 17(1):177–204, 2005.
- Hirotaka Nakayama, Yeboon Yun, and Min Yoon. *Sequential approximate multiobjective optimization using computational intelligence*. Springer Science & Business Media, 2009.
- Biswajit Paria, Kirthevasan Kandasamy, and B. Póczos. A flexible framework for multi-objective bayesian optimization using random scalarizations. In *UAI*, 2019.
- Victor Picheny. Multiobjective optimization using gaussian process emulators via stepwise uncertainty reduction. *Statistics and Computing*, 25(6):1265–1280, 2015.
- Wolfgang Ponweiser, Tobias Wagner, Dirk Biermann, and Markus Vincze. Multiobjective optimization on a limited budget of evaluations using model-assisted  $\mathcal{S}$ -metric selection. In *International Conference on Parallel Problem Solving from Nature*, pages 784–794. Springer, 2008.
- Carl Edward Rasmussen. Gaussian processes in machine learning. In *Summer School on Machine Learning*, pages 63–71. Springer, 2003.
- Ryan Rifkin, Sayan Mukherjee, Pablo Tamayo, Sridhar Ramaswamy, Chen-Hsiang Yeang, Michael Angelo, Michael Reich, Tomaso Poggio, Eric S Lander, Todd R Golub, et al. An analytical method for multiclass molecular cancer classification. *Siam Review*, 45(4):706–723, 2003.
- Diederik M Roijers, Peter Vamplew, Shimon Whiteson, and Richard Dazeley. A survey of multi-objective sequential decision-making. *Journal of Artificial Intelligence Research*, 48:67–113, 2013.
- Jonathan Scarlett, Ilija Bogunovic, and Volkan Cevher. Lower bounds on regret for noisy gaussian process bandit optimization. In *Conference on Learning Theory*, pages 1723–1742, 2017.
- Bobak Shahriari, Kevin Swersky, Ziyu Wang, Ryan P Adams, and Nando De Freitas. Taking the human out of the loop: A review of bayesian optimization. *Proceedings of the IEEE*, 104(1):148–175, 2015.

- Jasper Snoek, Hugo Larochelle, and Ryan P Adams. Practical bayesian optimization of machine learning algorithms. In *Advances in neural information processing systems*, pages 2951–2959, 2012.
- Niranjan Srinivas, Andreas Krause, Sham Kakade, and Matthias Seeger. Gaussian process optimization in the bandit setting: no regret and experimental design. In *Proceedings of the 27th International Conference on International Conference on Machine Learning*, pages 1015–1022. Omnipress, 2010.
- Kevin Swersky, Jasper Snoek, and Ryan P Adams. Multi-task bayesian optimization. In *Advances in neural information processing systems*, pages 2004–2012, 2013.
- Hans Wackernagel. *Multivariate geostatistics: an introduction with applications*. Springer Science & Business Media, 2013.
- Zi Wang, Clement Gehring, Pushmeet Kohli, and Stefanie Jegelka. Batched large-scale bayesian optimization in high-dimensional spaces. In *International Conference on Artificial Intelligence and Statistics*, pages 745–754, 2018.
- Indre Zliobaite. On the relation between accuracy and fairness in binary classification. *arXiv preprint arXiv:1505.05723*, 2015.
- Marcela Zuluaga, Guillaume Sergeant, Andreas Krause, and Markus Püschel. Active learning for multi-objective optimization. In *International Conference on Machine Learning*, pages 462–470, 2013.

# Appendix

## A Computational complexity under ICM kernels

In this section, we describe the time complexities of MT-KB and MT-BKB for the intrinsic coregionalization model (ICM)  $\Gamma(x, x') = k(x, x')B$ . As discussed earlier, we assume that an efficient oracle to optimize the acquisition function is provided to us, and the per step cost comes only from computing it. To this end, we first describe simplified model updates under ICM kernel using the eigen-system of  $B$  and then detail out the time required for computing the updates. We note here that the eigen decomposition, which is  $O(n^3)$ , needs to be computed only once at the beginning and can be used at every step of the algorithms.

**Per-step complexity of MT-KB** Let  $B = \sum_{i=1}^n \xi_i u_i u_i^\top$  denotes the eigen decomposition of the positive semi-definite matrix  $B$ . Then,  $\Gamma(x, x) = \sum_{i=1}^n \xi_i k(x, x) u_i u_i^\top$ . From the definition of the Kronecker product, we now have  $G_t = \sum_{i=1}^n \xi_i K_t \otimes u_i u_i^\top$  and  $G_t(x) = \sum_{i=1}^n \xi_i k_t(x) \otimes u_i u_i^\top$ , where  $K_t = [k(x_i, x_j)]_{i,j=1}^t$  and  $k_t(x) = [k(x_1, x), \dots, k(x_t, x)]^\top$ . Since  $\{u_i\}_{i=1}^n$  yields an orthonormal basis of  $\mathbb{R}^n$ , the output  $y_t \in \mathbb{R}^n$  can be written as  $y_t = \sum_{i=1}^n y_t^\top u_i \cdot u_i$ . We then have  $Y_t = \sum_{i=1}^n Y_t^i \otimes u_i$ , where  $Y_t^i = [y_1^\top u_i, \dots, y_t^\top u_i]^\top$ . We also note that  $I_{nt} = \sum_{i=1}^n I_t \otimes u_i u_i^\top$ , and, therefore  $G_t + \eta I_{nt} = \sum_{i=1}^n (\xi_i K_t + \eta I_t) \otimes u_i u_i^\top$ . Now, let  $K_t = \sum_{j=1}^t \alpha_j w_j w_j^\top$  denotes the eigen decomposition of the (positive semi-definite) kernel matrix  $K_t$ . We then have

$$G_t + \eta I_{nt} = \sum_{i=1}^n \sum_{j=1}^t (\xi_i \alpha_j + \eta) w_j w_j^\top \otimes u_i u_i^\top = \sum_{i=1}^n \sum_{j=1}^t (\xi_i \alpha_j + \eta) (w_j \otimes u_i) (w_j \otimes u_i)^\top. \quad (3)$$

By the properties of tensor product  $(w_j \otimes u_i)^\top (w_{j'} \otimes u_{i'}) = (w_j^\top w_{j'}) \cdot (u_i^\top u_{i'})$ , which is equal to 1 if  $i = i', j = j'$ , and is equal to 0 otherwise. Therefore, (3) denotes the eigen decomposition of  $G_t + \eta I_{nt}$ . Hence

$$(G_t + \eta I_{nt})^{-1} = \sum_{i=1}^n \sum_{j=1}^t \frac{1}{\xi_i \alpha_j + \eta} w_j w_j^\top \otimes u_i u_i^\top = \sum_{i=1}^n (\xi_i K_t + \eta I_t)^{-1} \otimes u_i u_i^\top. \quad (4)$$

By the orthonormality of  $\{u_i\}_{i=1}^n$  and the mixed product property of Kronecker product, we now obtain  $(G_t + \eta I_{nt})^{-1} Y_t = \sum_{i=1}^n (\xi_i K_t + \eta I_t)^{-1} Y_t^i \otimes u_i$ , and thus, in turn,

$$\mu_t(x) = G_t(x)^\top (G_t + \eta I_{nt})^{-1} Y_t = \sum_{i=1}^n \xi_i k_t(x)^\top (\xi_i K_t + \eta I_t)^{-1} Y_t^i \cdot u_i. \quad (5)$$

Similarly, we get  $G_t(x)^\top (G_t + \eta I_{nt})^{-1} G_t(x) = \sum_{i=1}^n \xi_i^2 k_t(x)^\top (\xi_i K_t + \eta I_t)^{-1} k_t(x) \cdot u_i u_i^\top$  and therefore,

$$\|\Gamma_t(x, x)\| = \max_{1 \leq i \leq n} \xi_i (k(x, x) - \xi_i k_t(x)^\top (\xi_i K_t + \eta I_t)^{-1} k_t(x)). \quad (6)$$

Let us now discuss the time required to compute  $\mu_t(x)$  and  $\|\Gamma_t(x, x)\|$ . Given the eigen decomposition, updating  $\{Y_t^i\}_{i=1}^n$  re-using those already computed at the previous step requires projecting the current output  $y_t$  onto all coordinates, and thus, takes  $O(n^2)$  time. Now, since the kernel matrix  $K_t$  is rescaled by the eigenvalues  $\xi_i$ , we can find the eigen decomposition of  $K_t$  once and reuse those to compute  $\{(\xi_i K_t + \eta I_t)^{-1}\}_{i=1}^n$  in  $O(t^3)$  time. Next, computing  $n$  matrix-vector multiplications and vector inner products of the form  $k_t(x)^\top (\xi_i K_t + \eta I_t)^{-1} k_t(x)$  and  $k_t(x)^\top (\xi_i K_t + \eta I_t)^{-1} Y_t^i$  take  $O(nt^2)$  time. Finally, the sum in (5) and the max in (6) can be computed in  $O(n^2)$  and  $O(n)$  time, respectively. Therefore, the overall cost to compute  $\mu_t(x)$  and  $\|\Gamma_t(x, x)\|$  are  $O(n^2 + nt^2 + t^3) = O(n^2 + t^2(n + t))$ .

**Per-step complexity of MT-BKB** Let  $\tilde{\varphi}_t(x) = \left(\tilde{K}_t^{1/2}\right)^+ \tilde{k}_t(x) \in \mathbb{R}^{m_t}$  denotes the Nyström embedding of the scalar kernel  $k$ , where  $\tilde{k}_t(x) = \left[\frac{1}{\sqrt{p_{t,i_1}}}k(x_{i_1}, x), \dots, \frac{1}{\sqrt{p_{t,i_{m_t}}}}k(x_{i_{m_t}}, x)\right]^\top$  and  $\tilde{K}_t = \left[\frac{1}{\sqrt{p_{t,i_u} p_{t,i_v}}}k(x_{i_u}, x_{i_v})\right]_{u,v=1}^{m_t}$ . Then the eigen decomposition  $B = \sum_{i=1}^n \xi_i u_i u_i^\top$  yields  $\tilde{G}_t = \sum_{i=1}^n \xi_i \tilde{K}_t \otimes u_i u_i^\top$  and  $\tilde{G}_t(x) = \sum_{i=1}^n \xi_i \tilde{k}_t(x) \otimes u_i u_i^\top$ . A similar argument as in (3) and (4) now implies  $\left(\tilde{G}_t^{1/2}\right)^+ = \sum_{i=1}^n \frac{1}{\sqrt{\xi_i}} \left(\tilde{K}_t^{1/2}\right)^+ \otimes u_i u_i^\top$ . Therefore, the Nyström embeddings for the multi-task kernel  $\Gamma$  can be computed using the embeddings for the scalar kernel  $k$  as

$$\tilde{\Phi}_t(x) = \left(\tilde{G}_t^{1/2}\right)^+ \tilde{G}_t(x) = \sum_{i=1}^n \sqrt{\xi_i} \left(\tilde{K}_t^{1/2}\right)^+ \tilde{k}_t(x) \otimes u_i u_i^\top = \sum_{i=1}^n \sqrt{\xi_i} \tilde{\varphi}_t(x) \otimes u_i u_i^\top.$$

We now have

$$\tilde{V}_t = \sum_{s=1}^t \tilde{\Phi}_t(x_s) \tilde{\Phi}_t(x_s)^\top = \sum_{s=1}^t \sum_{i=1}^n \xi_i \tilde{\varphi}_t(x_s) \tilde{\varphi}_t(x_s)^\top \otimes u_i u_i^\top = \sum_{i=1}^n \xi_i \tilde{v}_t \otimes u_i u_i^\top,$$

where  $\tilde{v}_t = \sum_{s=1}^t \tilde{\varphi}_t(x_s) \tilde{\varphi}_t(x_s)^\top$ . A similar argument as in (3) and (4) then implies

$$(\tilde{V}_t + \eta I_{nm_t})^{-1} = \sum_{i=1}^n (\xi_i \tilde{v}_t + \eta I_{m_t})^{-1} \otimes u_i u_i^\top.$$

We further have

$$\sum_{s=1}^t \tilde{\Phi}_t(x_s) y_s = \sum_{s=1}^t \sum_{i=1}^n \sqrt{\xi_i} y_s^\top u_i \tilde{\varphi}_t(x_s) \otimes u_i = \sum_{i=1}^n \sqrt{\xi_i} \left( \sum_{s=1}^t y_s^\top u_i \cdot \tilde{\varphi}_t(x_s) \right) \otimes u_i.$$

Similar to (5), we therefore obtain

$$\tilde{\mu}_t(x) = \sum_{i=1}^n \xi_i \tilde{\varphi}_t(x)^\top (\xi_i \tilde{v}_t + \eta I_{m_t})^{-1} \left( \sum_{s=1}^t y_s^\top u_i \cdot \tilde{\varphi}_t(x_s) \right) \cdot u_i. \quad (7)$$

We now note that  $\tilde{\Phi}_t(x)^\top \tilde{\Phi}_t(x) = \sum_{i=1}^n \xi_i \tilde{\varphi}_t(x)^\top \tilde{\varphi}_t(x) \cdot u_i u_i^\top$ . Similar to (6), we then obtain

$$\|\tilde{\Gamma}_t(x, x)\| = \max_{1 \leq i \leq n} \xi_i \left( k(x, x) - \tilde{\varphi}_t(x)^\top \tilde{\varphi}_t(x) + \eta \tilde{\varphi}_t(x)^\top (\xi_i \tilde{v}_t + \eta I_{m_t})^{-1} \tilde{\varphi}_t(x) \right). \quad (8)$$

We now discuss the time required to compute the scalar kernel embedding  $\tilde{\varphi}_t(x)$ . Sampling the dictionary  $\mathcal{D}_t$ , as we reuse the variances from the previous round, takes  $O(t)$  time. We now compute the embedding  $\tilde{\varphi}_t(x)$  in  $O(m_t^3 + m_t^2)$  time, which corresponds to an inversion of  $\tilde{K}_t^{1/2}$  and a matrix-vector product of dimension  $m_t$ , the size of the dictionary. Given the embedding function, let us now find the time required to compute  $\tilde{\mu}_t(x)$  and  $\|\tilde{\Gamma}_t(x, x)\|$ . We first construct the matrix  $\tilde{v}_t$  from scratch using all the points selected so far, which takes  $O(m_t^2 t)$  time. Then the inverses  $\{(\xi_i \tilde{v}_t + \eta I_{m_t})^{-1}\}_{i=1}^n$  can be computed in  $O(m_t^3)$  time and the matrix-vector multiplications  $\{(\xi_i \tilde{v}_t + \eta I_{m_t})^{-1} \tilde{\varphi}_t(x)\}_{i=1}^n$  in  $O(n m_t^2)$  time. Similar to MT-KB, projecting the current output onto every direction takes  $O(n^2)$  time. The projections can then be used to compute  $n$  vectors of the form  $\sum_{s=1}^t y_s^\top u_i \cdot \tilde{\varphi}_t(x_s)$  in  $O(n m_t t)$  time. Finally,  $n$  vector inner products of dimension  $m_t$  can be computed in  $O(n m_t)$  time. Therefore, the overall cost to compute (7) and (8) is  $O(n^2 + n m_t t + n m_t^2 + m_t^3 + m_t^2 t) = O(n^2 + m_t t(n + t))$ , since the dictionary size  $m_t \leq t$ .

## B Multi-task concentration

We first introduce some notations. For any two Hilbert spaces  $\mathcal{G}$  and  $\mathcal{H}$  with respective inner products  $\langle \cdot, \cdot \rangle_{\mathcal{G}}$  and  $\langle \cdot, \cdot \rangle_{\mathcal{H}}$ , we denote by  $\mathcal{L}(\mathcal{G}, \mathcal{H})$  the space of all bounded linear operators from  $\mathcal{G}$  to  $\mathcal{H}$ , with the operator norm  $\|A\| := \sup_{\|g\|_{\mathcal{G}} \leq 1} \|Ag\|_{\mathcal{H}}$ . We also denote, for any  $A \in \mathcal{L}(\mathcal{G}, \mathcal{H})$ , by  $A^\top$  its adjoint, which is the unique operator such that  $\langle A^\top h, g \rangle_{\mathcal{G}} = \langle h, Ag \rangle_{\mathcal{H}}$  for all  $g \in \mathcal{G}$ ,  $h \in \mathcal{H}$ . In the case  $\mathcal{G} = \mathcal{H}$ , we denote  $\mathcal{L}(\mathcal{H}) = \mathcal{L}(\mathcal{H}, \mathcal{H})$ . We now review the following lemma (Rasmussen, 2003) about operators, which we will use several times.

**Lemma 2 (Operator identities)** *Let  $A \in \mathcal{L}(\mathcal{G}, \mathcal{H})$ . Then, for any  $\eta > 0$ , the following hold*

$$\begin{aligned} (A^\top A + \eta I)^{-1} A^\top &= A^\top (A A^\top + \eta I)^{-1}, \\ I - A^\top (A A^\top + \eta I)^{-1} A &= \eta (A^\top A + \eta I)^{-1}. \end{aligned}$$

We now present the main result of this appendix, which is stated and proved using the feature map of the multi-task kernel.

**Feature map of multi-task kernel** We assume the multi-task kernel  $\Gamma$  to be continuous relative to the operator norm on  $\mathcal{L}(\mathbb{R}^n)$ , the space of bounded linear operators from  $\mathbb{R}^n$  to itself. Then the RKHS  $\mathcal{H}_\Gamma(\mathcal{X})$  associated with the kernel  $\Gamma$  is a subspace of the space of continuous functions from  $\mathcal{X}$  to  $\mathbb{R}^n$ , and hence,  $\Gamma$  is a Mercer kernel (Carmeli et al., 2010). Let  $\mu$  be a probability measure on the (compact) set  $\mathcal{X}$ . Since  $\Gamma$  is a Mercer kernel on  $\mathcal{X}$  and  $\sup_{x \in \mathcal{X}} \|\Gamma(x, x)\| < \infty$ , the RKHS  $\mathcal{H}_\Gamma(\mathcal{X})$  is

a subspace of  $L^2(\mathcal{X}, \mu; \mathbb{R}^n)$ , the Banach space of measurable functions  $g : \mathcal{X} \rightarrow \mathbb{R}^n$  such that  $\int_{\mathcal{X}} \|g(x)\|^2 d\mu(x) < \infty$ , with norm  $\|g\|_{L^2} = \left(\int_{\mathcal{X}} \|g(x)\|^2 d\mu(x)\right)^{1/2}$ . Since  $\Gamma(x, x) \in \mathcal{L}(\mathbb{R}^n)$  is a compact operator<sup>6</sup>, by the Mercer theorem for multi-task kernels (Carmeli et al., 2010), there exists an at most countable sequence  $\{(\psi_i, \nu_i)\}_{i \in \mathbb{N}}$  such that

$$\Gamma(x, x') = \sum_{i=1}^{\infty} \nu_i \psi_i(x) \psi_i(x')^\top \quad \text{and}$$

$$\|g\|_{\Gamma}^2 = \sum_{i=1}^{\infty} \frac{\langle g, \psi_i \rangle_{L^2}^2}{\nu_i}, \quad g \in L^2(\mathcal{X}, \mu; \mathbb{R}^n),$$

where  $\nu_i \geq 0$  for all  $i$ ,  $\lim_{i \rightarrow \infty} \nu_i = 0$  and  $\{\psi_i : \mathcal{X} \rightarrow \mathbb{R}^n\}_{i \in \mathbb{N}}$  is an orthonormal basis of  $L^2(\mathcal{X}, \mu; \mathbb{R}^n)$ . In particular  $g \in \mathcal{H}_{\Gamma}(\mathcal{X})$  if and only if  $\|g\|_{\Gamma} < \infty$ . Note that  $\{\sqrt{\nu_i} \psi_i\}_{i \in \mathbb{N}}$  is an orthonormal basis of  $\mathcal{H}_{\Gamma}(\mathcal{X})$ . Then, we can represent the objective function  $f \in \mathcal{H}_{\Gamma}(\mathcal{X})$  as

$$f = \sum_{i=1}^{\infty} \theta_i^* \sqrt{\nu_i} \psi_i$$

for some  $\theta^* := (\theta_1^*, \theta_2^*, \dots) \in \ell^2$ , the Hilbert space of square-summable sequences of real numbers, such that  $\|f\|_{\Gamma} = \|\theta^*\|_2 := (\sum_{i=1}^{\infty} |\theta_i^*|^2)^{1/2} < \infty$ . We now define a feature map  $\Phi : \mathcal{X} \rightarrow \mathcal{L}(\mathbb{R}^n, \ell^2)$  of the multi-task kernel  $\Gamma$  by

$$\Phi(x)y := (\sqrt{\nu_1} \psi_1(x)^\top y, \sqrt{\nu_2} \psi_2(x)^\top y, \dots), \quad \forall x \in \mathcal{X}, y \in \mathbb{R}^n.$$

We then have  $f(x) = \Phi(x)^\top \theta^*$  and  $\Gamma(x, x') = \Phi(x)^\top \Phi(x')$  for all  $x, x' \in \mathcal{X}$ .

**Martingale control in  $\ell^2$  space** Let us define  $S_t = \sum_{s=1}^t \Phi(x_s) \varepsilon_s$ , where  $\varepsilon_1, \dots, \varepsilon_t$  are the random noise vectors in  $\mathbb{R}^n$ . Now consider  $\mathcal{F}_{t-1}$ , the  $\sigma$ -algebra generated by the random variables  $\{x_s, \varepsilon_s\}_{s=1}^{t-1}$  and  $x_t$ . Observe that  $S_t$  is  $\mathcal{F}_t$ -measurable and  $\mathbb{E}[S_t \mid \mathcal{F}_{t-1}] = S_{t-1}$ . The process  $\{S_t\}_{t \geq 1}$  is thus a martingale with values<sup>7</sup> in the  $\ell^2$  space. We now define a map  $\Phi_{\mathcal{X}_t} : \ell^2 \rightarrow \mathbb{R}^{nt}$  by

$$\Phi_{\mathcal{X}_t} \theta := \left[ (\Phi(x_1)^\top \theta)^\top, \dots, (\Phi(x_t)^\top \theta)^\top \right]^\top, \quad \forall \theta \in \ell^2.$$

We also let  $V_t := \Phi_{\mathcal{X}_t}^\top \Phi_{\mathcal{X}_t}$  be a map from  $\ell^2$  to itself and  $I$  be the identity operator in  $\ell^2$ . In Lemma 3, we measure the deviation of  $S_t$  by the norm weighted by  $(V_t + \eta I)^{-1}$ , which is itself derived from  $S_t$ . Lemma 3 represents the multi-task generalization of the result of Durand et al. (2018), and we recover their result under the single-task setting ( $n = 1$ ).

<sup>6</sup>An operator  $A \in \mathcal{L}(\mathcal{H})$  is said to be compact if the image of each bounded set under  $A$  is relatively compact.

<sup>7</sup>We ignore issues of measurability here.



**Lemma 3 (Self-normalized martingale control)** *Let the noise vectors  $\{\varepsilon_t\}_{t \geq 1}$  be  $\sigma$ -sub-Gaussian. Then, for any  $\eta > 0$  and  $\delta \in (0, 1]$ , with probability at least  $1 - \delta$ , the following holds uniformly over all  $t \geq 1$ :*

$$\|S_t\|_{(V_t + \eta I)^{-1}} \leq \sigma \sqrt{2 \log(1/\delta) + \log \det(I + \eta^{-1} V_t)}.$$

**Proof** For any sequence of real numbers  $\theta = (\theta_1, \theta_2, \dots)$  such that  $\|\sum_{i=1}^{\infty} \theta_i \sqrt{\nu_i} \psi_i(x)\|_2 < \infty$ , let us define  $\Phi(x)^\top \theta := \sum_{i=1}^{\infty} \theta_i \sqrt{\nu_i} \psi_i(x)$  and

$$M_t^\theta = \prod_{s=1}^t D_s^\theta, \quad D_s^\theta = \exp\left(\frac{\varepsilon_s^\top \Phi(x_s)^\top \theta}{\sigma} - \frac{1}{2} \|\Phi(x_s)^\top \theta\|_2^2\right).$$

Since the noise vectors  $\{\varepsilon_t\}_{t \geq 1}$  are conditionally  $\sigma$ -sub-Gaussian, i.e.,

$$\forall \alpha \in \mathbb{R}^n, \forall t \geq 1, \quad \mathbb{E}[\exp(\varepsilon_t^\top \alpha) \mid \mathcal{F}_{t-1}] \leq \exp\left(\sigma^2 \|\alpha\|_2^2 / 2\right),$$

we have  $\mathbb{E}[D_t^\theta \mid \mathcal{F}_{t-1}] \leq 1$  and hence  $\mathbb{E}[M_t^\theta \mid \mathcal{F}_{t-1}] \leq M_{t-1}^\theta$ . Therefore, it is immediate that  $\{M_t^\theta\}_{t=0}^\infty$  is a non-negative super-martingale and actually satisfies  $\mathbb{E}[M_t^\theta] \leq 1$ .

Now, let  $\tau$  be a stopping time with respect to the filtration  $\{\mathcal{F}_t\}_{t=0}^\infty$ . By the convergence theorem for non-negative super-martingales,  $M_\infty^\theta = \lim_{t \rightarrow \infty} M_t^\theta$  is almost surely well-defined, and thus  $M_\tau^\theta$  is well-defined as well irrespective of whether  $\tau < \infty$  or not. Let  $Q_t^\theta = M_{\min\{\tau, t\}}^\theta$  be a stopped version of  $\{M_t^\theta\}_t$ . Then, by Fatou's lemma,

$$\mathbb{E}[M_\tau^\theta] = \mathbb{E}\left[\liminf_{t \rightarrow \infty} Q_t^\theta\right] \leq \liminf_{t \rightarrow \infty} \mathbb{E}[Q_t^\theta] = \liminf_{t \rightarrow \infty} \mathbb{E}[M_{\min\{\tau, t\}}^\theta] \leq 1, \quad (9)$$

since the stopped super-martingale  $\{M_{\min\{\tau, t\}}^\theta\}_{t \geq 1}$  is also a super-martingale.

Let  $\mathcal{F}_\infty$  be the  $\sigma$ -algebra generated by  $\{\mathcal{F}_t\}_{t=0}^\infty$ , and  $\Theta = (\Theta_1, \Theta_2, \dots)$ ,  $\Theta_i \sim \mathcal{N}(0, 1/\eta)$  be an infinite i.i.d. Gaussian random sequence which is independent of  $\mathcal{F}_\infty$ . Since  $\Gamma(x, x) \in \mathcal{L}(\mathbb{R}^n)$  has finite trace, we have

$$\mathbb{E}\left[\left\|\sum_{i=1}^{\infty} \Theta_i \sqrt{\nu_i} \psi_i(x)\right\|_2^2\right] = \frac{1}{\eta} \sum_{i=1}^{\infty} \nu_i \|\psi_i(x)\|_2^2 = \frac{1}{\eta} \text{trace}(\Gamma(x, x)) < \infty.$$

Therefore,  $\|\sum_{i=1}^{\infty} \Theta_i \sqrt{\nu_i} \psi_i(x)\|_2 < \infty$  almost surely and thus  $M_t^\Theta$  is well-defined. Now, thanks to the sub-Gaussian property,  $\mathbb{E}[M_t^\Theta \mid \Theta] \leq 1$  almost surely, and thus  $\mathbb{E}[M_t^\Theta] \leq 1$  for all  $t$ .

Let  $M_t := \mathbb{E}[M_t^\Theta \mid \mathcal{F}_\infty]$  be a mixture of non-negative super-martingales  $M_t^\Theta$ . Then  $\{M_t\}_{t=0}^\infty$  is also a non-negative super-martingale adapted to the filtration  $\{\mathcal{F}_t\}_{t=0}^\infty$ . Hence, by a similar argument as in (9),  $M_\tau$  is almost surely well-defined and  $\mathbb{E}[M_\tau] = \mathbb{E}[M_\tau^\Theta] \leq 1$ . Let us now compute the mixture martingale  $M_t$ . We first note for any  $\theta \in \ell^2$  that  $M_t^\theta = \exp\left(\langle \theta, S_t / \sigma \rangle_2 - \frac{1}{2} \|\theta\|_{V_t}^2\right)$ . The difficulty however lies in the

handling of possibly infinite dimension. To this end, we follow Durand et al. (2018) to consider the first  $d$  dimensions for each  $d \in \mathbb{N}$ . Let  $\Theta_d$  denote the restriction of  $\Theta$  to the first  $d$  components. Thus  $\Theta_d \sim \mathcal{N}(0, \frac{1}{\eta} I_d)$ . Similarly, let  $S_{t,d}$ ,  $V_{t,d}$  and  $M_{t,d}$  denote the corresponding restrictions of  $S_t$ ,  $V_t$  and  $M_t$ , respectively. Following the steps from Chowdhury and Gopalan (2017), we then obtain that

$$\begin{aligned} M_{t,d} &= \frac{\det(\eta I_d)^{1/2}}{(2\pi)^{d/2}} \int_{\mathbb{R}^d} \exp\left(\langle \alpha, S_{t,d}/\sigma \rangle_2 - \frac{1}{2} \|\alpha\|_{V_{t,d}}^2\right) \exp\left(-\frac{\eta}{2} \|\alpha\|_2^2\right) d\alpha \\ &= \frac{1}{\det(I_d + \eta^{-1} V_{t,d})^{1/2}} \exp\left(\frac{1}{2\sigma^2} \|S_{t,d}\|_{(V_{t,d} + \eta I_d)^{-1}}^2\right). \end{aligned}$$

Note that  $M_{\tau,d}$  is also almost surely well defined and  $\mathbb{E}[M_{\tau,d}] \leq 1$  for all  $d \in \mathbb{N}$ . We now fix a  $\delta \in (0, 1]$ . An application of Markov's inequality and Fatou's Lemma then yields

$$\begin{aligned} \mathbb{P}\left[\|S_\tau\|_{(V_\tau + \eta I)^{-1}}^2 > 2\sigma^2 \log\left(\frac{\det(I + \eta^{-1} V_\tau)^{1/2}}{\delta}\right)\right] &= \mathbb{P}\left[\frac{\exp\left(\frac{1}{2\sigma^2} \|S_\tau\|_{(V_\tau + \eta I)^{-1}}^2\right)}{\frac{1}{\delta} \det(I + \eta^{-1} V_\tau)^{1/2}} > 1\right] \\ &= \mathbb{P}\left[\lim_{d \rightarrow \infty} \frac{\exp\left(\frac{1}{2\sigma^2} \|S_{\tau,d}\|_{(V_{\tau,d} + \eta I_d)^{-1}}^2\right)}{\frac{1}{\delta} \det(I_d + \eta^{-1} V_{\tau,d})^{1/2}} > 1\right] \\ &\leq \mathbb{E}\left[\lim_{d \rightarrow \infty} \frac{\exp\left(\frac{1}{2\sigma^2} \|S_{\tau,d}\|_{(V_{\tau,d} + \eta I_d)^{-1}}^2\right)}{\frac{1}{\delta} \det(I_d + \eta^{-1} V_{\tau,d})^{1/2}}\right] \\ &\leq \delta \lim_{d \rightarrow \infty} \mathbb{E}[M_{\tau,d}] \leq \delta. \end{aligned}$$

We now define a random stopping time  $\tau$  following Chowdhury and Gopalan (2017), by

$$\tau = \min\left\{t \geq 0 : \|S_t\|_{(V_t + \eta I)^{-1}}^2 > 2\sigma^2 \log\left(\frac{\det(I + \eta^{-1} V_t)^{1/2}}{\delta}\right)\right\}.$$

We then have

$$\mathbb{P}\left[\exists t \geq 1 : \|S_t\|_{(V_t + \eta I)^{-1}}^2 > 2\sigma^2 \log\left(\frac{\det(I + \eta^{-1} V_t)^{1/2}}{\delta}\right)\right] = \mathbb{P}[\tau < \infty] \leq \delta,$$

which concludes the proof. ■

### B.1 Concentration bound for the estimate (Proof of Theorem 1)

We first reformulate  $\mu_t(x)$  in terms of the feature map  $\Phi(x)$  as

$$\begin{aligned}
\mu_t(x) &= G_t(x)^\top (G_t + \eta I_{nt})^{-1} Y_t \\
&= \Phi(x)^\top \Phi_{\mathcal{X}_t}^\top (\Phi_{\mathcal{X}_t} \Phi_{\mathcal{X}_t}^\top + \eta I_{nt})^{-1} Y_t \\
&= \Phi(x)^\top (\Phi_{\mathcal{X}_t}^\top \Phi_{\mathcal{X}_t} + \eta I)^{-1} \Phi_{\mathcal{X}_t}^\top Y_t \\
&= \Phi(x)^\top (V_t + \eta I)^{-1} \sum_{s=1}^t \Phi(x_s) y_s \\
&= \Phi(x)^\top (V_t + \eta I)^{-1} \sum_{s=1}^t \Phi(x_s) (f(x_s) + \varepsilon_s) \\
&= \Phi(x)^\top (V_t + \eta I)^{-1} \sum_{s=1}^t \Phi(x_s) (\Phi(x_s)^\top \theta^* + \varepsilon_s) \\
&= \Phi(x)^\top \theta^* - \eta \Phi(x)^\top (V_t + \eta I)^{-1} \theta^* + \Phi(x)^\top (V_t + \eta I)^{-1} S_t \\
&= f(x) + \Phi(x)^\top (V_t + \eta I)^{-1} (S_t - \eta \theta^*),
\end{aligned}$$

where the third step follows from Lemma 2. We now obtain, from the definition of operator norm, the following

$$\begin{aligned}
\|f(x) - \mu_t(x)\|_2 &\leq \left\| \Phi(x)^\top (V_t + \eta I)^{-1/2} \right\| \left\| (V_t + \eta I)^{-1/2} (S_t - \eta \theta^*) \right\|_2 \\
&\leq \left\| (V_t + \eta I)^{-1/2} \Phi(x) \right\| \left( \|S_t\|_{(V_t + \eta I)^{-1}} + \eta \|\theta^*\|_{(V_t + \eta I)^{-1}} \right) \\
&\leq \left\| \Phi(x)^\top (V_t + \eta I)^{-1} \Phi(x) \right\|^{1/2} \left( \|S_t\|_{(V_t + \eta I)^{-1}} + \eta^{1/2} \|f\|_\Gamma \right),
\end{aligned}$$

where the last step is controlled as  $\|\theta^*\|_{(V_t + \eta I)^{-1}} \leq \eta^{-1/2} \|\theta^*\|_2 = \eta^{-1/2} \|f\|_\Gamma$ . A simple application of Lemma 2 now yields

$$\begin{aligned}
\eta \Phi(x)^\top (V_t + \eta I)^{-1} \Phi(x) &= \eta \Phi(x)^\top (\Phi_{\mathcal{X}_t}^\top \Phi_{\mathcal{X}_t} + \eta I)^{-1} \Phi(x) \\
&= \Phi(x)^\top \Phi(x) - \Phi(x)^\top \Phi_{\mathcal{X}_t}^\top (\Phi_{\mathcal{X}_t} \Phi_{\mathcal{X}_t}^\top + \eta I_{nt})^{-1} \Phi_{\mathcal{X}_t} \Phi(x) \\
&= \Gamma(x, x) - G_t(x)^\top (G_t + \eta I_{nt})^{-1} G_t(x) = \Gamma_t(x, x). \quad (10)
\end{aligned}$$

We then have  $\left\| \Phi(x)^\top (V_t + \eta I)^{-1} \Phi(x) \right\|^{1/2} = \eta^{-1/2} \|\Gamma_t(x, x)\|^{1/2}$ . We conclude the proof from Lemma 3 and using Sylvester's identity to get

$$\det(I + \eta^{-1} V_t) = \det(I + \eta^{-1} \Phi_{\mathcal{X}_t}^\top \Phi_{\mathcal{X}_t}) = \det(I_{nt} + \eta^{-1} \Phi_{\mathcal{X}_t} \Phi_{\mathcal{X}_t}^\top) = \det(I_{nt} + \eta^{-1} G_t). \quad (11)$$

## C Regret analysis of MT-KB

### C.1 Properties of predictive variance

**Lemma 4 (Sum of predictive variances)** *For any  $\eta > 0$  and  $t \geq 1$ ,*

$$\frac{1}{\eta} \sum_{s=1}^t \text{trace}(\Gamma_s(x_s, x_s)) = \log \det(I_{nt} + \eta^{-1} G_t) = \sum_{s=1}^t \log \det(I_n + \eta^{-1} \Gamma_{s-1}(x_s, x_s)).$$

**Proof** For the first part, we observe from (10) that

$$\begin{aligned} \frac{1}{\eta} \sum_{s=1}^t \text{trace}(\Gamma_s(x_s, x_s)) &= \sum_{s=1}^t \text{trace}(\Phi(x_s)^\top (V_s + \eta I)^{-1} \Phi(x_s)) \\ &= \sum_{s=1}^t \text{trace}((V_s + \eta I)^{-1} \Phi(x_s) \Phi(x_s)^\top) \\ &= \sum_{s=1}^t \text{trace}((V_s + \eta I)^{-1} ((V_s + \eta I) - (V_{s-1} + \eta I))) \\ &\leq \sum_{s=1}^t \log \left( \frac{\det(V_s + \eta I)}{\det(V_{s-1} + \eta I)} \right) \\ &= \log \det(I + \eta^{-1} V_t) = \log \det(I_{nt} + \eta^{-1} G_t). \end{aligned}$$

Here, the last equality follows from (11). The inequality follows from the fact that for two p.d. matrices  $A$  and  $B$  such that  $A - B$  is p.s.d.,  $\text{trace}(A^{-1}(A - B)) \leq \log \left( \frac{\det(A)}{\det(B)} \right)$  (Calandriello et al., 2019).

For the second part, we obtain from Schur's determinant identity that

$$\begin{aligned} &\det(I_{nt} + \eta^{-1} G_t) \\ &= \det(I_{n(t-1)} + \eta^{-1} G_{t-1}) \times \\ &\quad \det \left( I_n + \eta^{-1} \Gamma(x_t, x_t) - \eta^{-1} G_{t-1}(x_t)^\top (I_{n(t-1)} + \eta^{-1} G_{t-1})^{-1} \eta^{-1} G_{t-1}(x_t) \right) \\ &= \det(I_{n(t-1)} + \eta^{-1} G_{t-1}) \det(I_n + \eta^{-1} \Gamma_{t-1}(x_t, x_t)) \\ &= \dots \\ &= \prod_{s=1}^t \det(I_n + \eta^{-1} \Gamma_{s-1}(x_s, x_s)). \end{aligned}$$

We conclude the proof by applying logarithm on both sides. ■

**Lemma 5 (Predictive variance geometry)** *Let  $\|\Gamma(x, x)\| \leq \kappa$ . Then, for any  $\eta > 0$  and  $t \geq 1$ ,*

$$\Gamma_t(x, x) \preceq \Gamma_{t-1}(x, x) \preceq (1 + \kappa/\eta) \Gamma_t(x, x).$$

**Proof** Let us define  $\bar{V}_t = V_t + \eta I$  for all  $t \geq 0$ . We then have from (10) that

$$\begin{aligned}
\Gamma_t(x, x) &= \eta \Phi(x)^\top \bar{V}_t^{-1} \Phi(x) \\
&= \eta \Phi(x)^\top (\bar{V}_{t-1} + \Phi(x_t) \Phi(x_t)^\top)^{-1} \Phi(x) \\
&= \eta \Phi(x)^\top \bar{V}_{t-1}^{-1} \Phi(x) - \\
&\quad \eta \Phi(x)^\top \bar{V}_{t-1}^{-1} \Phi(x_t) \left( I_n + \Phi(x_t)^\top \bar{V}_{t-1}^{-1} \Phi(x_t) \right)^{-1} \Phi(x_t)^\top \bar{V}_{t-1}^{-1} \Phi(x) \\
&= \Gamma_{t-1}(x, x) - \eta^{-1} \Gamma_{t-1}(x_t, x)^\top (I_n + \eta^{-1} \Gamma_{t-1}(x_t, x_t))^{-1} \Gamma_{t-1}(x_t, x) \\
&\preceq \Gamma_{t-1}(x, x).
\end{aligned}$$

Here in the third step, we have used the Sherman-Morrison formula and in the last step, we have used the positive semi-definite property of multi-task kernels. To prove the second part, we first note that

$$\begin{aligned}
\frac{1}{\eta} \Gamma_t(x, x) &= \Phi(x)^\top (\bar{V}_{t-1} + \Phi(x_t) \Phi(x_t)^\top)^{-1} \Phi(x) \\
&= \Phi(x)^\top \bar{V}_{t-1}^{-1/2} \left( I + \bar{V}_{t-1}^{-1/2} \Phi(x_t) \Phi(x_t)^\top \bar{V}_{t-1}^{-1/2} \right)^{-1} \bar{V}_{t-1}^{-1/2} \Phi(x) \quad (12)
\end{aligned}$$

Further, since  $\|\Gamma(x, x)\| \leq \kappa$ , we have  $\lambda_{\max}(\Gamma(x, x)) \leq \kappa$ , and hence,

$$\Gamma_t(x, x) \preceq \Gamma_{t-1}(x, x) \preceq \Gamma_{t-2}(x, x) \preceq \dots \Gamma_0(x, x) = \Gamma(x, x) \preceq \kappa I_n. \quad (13)$$

Since  $\bar{V}_{t-1}^{-1/2} \Phi(x_t) \Phi(x_t)^\top \bar{V}_{t-1}^{-1/2}$  and  $\Phi(x_t)^\top \bar{V}_{t-1}^{-1} \Phi(x_t)$  have same set of non-zero eigenvalues, we now obtain from (13) that  $\bar{V}_{t-1}^{-1/2} \Phi(x_t) \Phi(x_t)^\top \bar{V}_{t-1}^{-1/2} \preceq \frac{\kappa}{\eta} I$ . Then (12) implies that

$$\Gamma_t(x, x) \succeq \eta \Phi(x)^\top \bar{V}_{t-1}^{-1} \Phi(x) / (1 + \kappa/\eta) = \Gamma_{t-1}(x, x) / (1 + \kappa/\eta),$$

which completes the proof.  $\blacksquare$

## C.2 Regret bound for MT-KB (Proof of Theorem 2)

Since the scalarization functions  $s_\lambda$  is  $L_\lambda$ -Lipschitz in the  $\ell_2$  norm, we have

$$|s_{\lambda_t}(f(x)) - s_{\lambda_t}(\mu_{t-1}(x))| \leq L_{\lambda_t} \|f(x) - \mu_{t-1}(x)\|_2.$$

Since  $\mu_0(x) = 0$ ,  $\Gamma_0(x, x) = \Gamma(x, x)$  and  $\|f\|_\Gamma \leq b$ , we have

$$\|f(x) - \mu_0(x)\|_2 = \|\Gamma_x^\top f\|_2 \leq \|f\|_\Gamma \|\Gamma_x\| = \|f\|_\Gamma \|\Gamma_x^\top \Gamma_x\|^{1/2} \leq b \|\Gamma_0(x, x)\|^{1/2}.$$

Then, from Theorem 1 and Lemma 4, the following holds with probability at least  $1 - \delta$ :

$$\forall t \geq 1, \forall x \in \mathcal{X}, \quad |s_{\lambda_t}(f(x)) - s_{\lambda_t}(\mu_{t-1}(x))| \leq L_{\lambda_t} \beta_{t-1} \|\Gamma_{t-1}(x, x)\|^{1/2}, \quad (14)$$

where  $\beta_t = b + \frac{\sigma}{\sqrt{\eta}} \sqrt{2 \log(1/\delta) + \sum_{s=1}^t \log \det(I_n + \eta^{-1} \Gamma_{s-1}(x_s, x_s))}$ ,  $t \geq 0$ . We can now upper bound the *instantaneous regret* at time  $t \geq 1$  as

$$\begin{aligned} r_{\lambda_t}(x_t) &:= s_{\lambda_t}(f(x_{\lambda_t}^*)) - s_{\lambda_t}(f(x_t)) \\ &\leq s_{\lambda_t}(\mu_{t-1}(x_{\lambda_t}^*)) + L_{\lambda_t} \beta_{t-1} \|\Gamma_{t-1}(x_{\lambda_t}^*, x_{\lambda_t}^*)\|^{1/2} - s_{\lambda_t}(f(x_t)) \\ &\leq s_{\lambda_t}(\mu_{t-1}(x_t)) + L_{\lambda_t} \beta_{t-1} \|\Gamma_{t-1}(x_t, x_t)\|^{1/2} - s_{\lambda_t}(f(x_t)) \\ &\leq 2L_{\lambda_t} \beta_{t-1} \|\Gamma_{t-1}(x_t, x_t)\|^{1/2}. \end{aligned}$$

Here in the first and third step, we have used (14). The second step follows from the choice of  $x_t$ . Since  $\beta_t$  is a monotonically increasing function in  $t$  and  $L_{\lambda_t} \leq L$  for all  $t$ , we have

$$\sum_{t=1}^T r_{\lambda_t}(x_t) \leq 2L\beta_T \sum_{t=1}^T \|\Gamma_{t-1}(x_t, x_t)\|^{1/2} \leq 2L\beta_T \sqrt{(1 + \kappa/\eta)T \sum_{t=1}^T \|\Gamma_t(x_t, x_t)\|},$$

where the last step is due to the Cauchy-Schwartz inequality and Lemma 5. We now obtain from Lemma 4 that  $\beta_T \leq b + \frac{\sigma}{\sqrt{\eta}} \sqrt{2(\log(1/\delta) + \gamma_{nT}(\Gamma, \eta))}$ . We conclude the proof by taking an expectation over  $\{\lambda_i\}_{i=1}^T \sim P_\lambda$ .

### C.3 Inter-task structure in regret for separable kernels (Proof of Lemma 1)

For separable multi-task kernels  $\Gamma(x, x') = k(x, x')B$ , the kernel matrix is given by  $G_T = K_T \otimes B$ , where  $K_T$  is kernel matrix corresponding to the scalar kernel  $k$  and  $\otimes$  denotes the Kronecker product. Let  $\{\alpha_t\}_{t=1}^T$  denote the eigenvalues of  $K_T$ . Then the eigenvalues of  $G_T$  are given by  $\alpha_t \xi_i$ ,  $1 \leq t \leq T$ ,  $1 \leq i \leq n$ , where  $\xi_i$ 's are the eigenvalues of  $B$ . We now have

$$\begin{aligned} \log \det(I_{nT} + \eta^{-1} G_T) &= \sum_{t=1}^T \sum_{i=1}^n \log(1 + \alpha_t \xi_i / \eta) \\ &= \sum_{i \in [n]: \xi_i > 0} \sum_{t=1}^T \log(1 + \alpha_t \xi_i / \eta) \\ &= \sum_{i \in [n]: \xi_i > 0} \log \det(I_T + (\eta / \xi_i)^{-1} K_T). \end{aligned}$$

Taking supremum over all possible subsets  $\mathcal{X}_T$  of  $\mathcal{X}$ , we then obtain that  $\gamma_{nT}(\Gamma, \eta) \leq \sum_{i \in [n]: \xi_i > 0} \gamma_T(k, \eta / \xi_i)$ .

To prove the second part, we use the feature representation of the scalar kernel  $k$ . To this end, we let  $\varphi : \mathcal{X} \rightarrow \ell^2$  be a feature map of the scalar kernel  $k$ , so that  $k(x, x') = \varphi(x)^\top \varphi(x')$  for all  $x, x' \in \mathcal{X}$ . We now define a map  $\varphi_{\mathcal{X}_t} : \ell^2 \rightarrow \mathbb{R}^t$  by

$$\varphi_{\mathcal{X}_t} \theta := [\varphi(x_1)^\top \theta, \dots, \varphi(x_t)^\top \theta]^\top, \quad \forall \theta \in \ell^2.$$

We also let  $v_t := \varphi_{\mathcal{X}_t}^\top \varphi_{\mathcal{X}_t}$  be a map from  $\ell^2$  to itself. For any  $\alpha > 0$ , we then obtain from Lemma 2 that

$$\begin{aligned} \alpha \varphi(x)^\top (v_t + \alpha I)^{-1} \varphi(x) &= \alpha \varphi(x)^\top (\varphi_{\mathcal{X}_t}^\top \varphi_{\mathcal{X}_t} + \alpha I)^{-1} \varphi(x) \\ &= \varphi(x)^\top \varphi(x) - \varphi(x)^\top \varphi_{\mathcal{X}_t}^\top (\varphi_{\mathcal{X}_t} \varphi_{\mathcal{X}_t}^\top + \alpha I_t)^{-1} \varphi_{\mathcal{X}_t} \varphi(x) \\ &= k(x, x) - k_t(x)^\top (K_t + \alpha I_t)^{-1} k_t(x), \end{aligned}$$

where  $k_t(x) = [k(x_1, x), \dots, k(x_t, x)]^\top$  and  $K_t = [k(x_i, x_j)]_{i,j=1}^t$ . We then have from (6) that

$$\begin{aligned} \|\Gamma_t(x, x)\| &= \max_{1 \leq i \leq n} \xi_i \left( k(x, x) - k_t(x)^\top \left( K_t + \frac{\eta}{\xi_i} I_t \right)^{-1} k_t(x) \right) \\ &= \max_{1 \leq i \leq n} \xi_i \cdot \frac{\eta}{\xi_i} \varphi(x)^\top \left( v_t + \frac{\eta}{\xi_i} I \right)^{-1} \varphi(x) \\ &\leq \eta \varphi(x)^\top \left( v_t + \frac{\eta}{\kappa} I \right)^{-1} \varphi(x). \end{aligned}$$

Here, in the last step we have used that  $\xi_i \leq \kappa$  for all  $i \in [n]$ . This holds from our hypothesis  $\|\Gamma(x, x)\| \leq \kappa$  and  $k(x, x) = 1$ . We now observe that  $(v_t + \frac{\eta}{\kappa} I)^{-1} \preceq (v_t + \eta I)^{-1}$  for  $\kappa \leq 1$  and  $(v_t + \frac{\eta}{\kappa} I)^{-1} \preceq \kappa (v_t + \eta I)^{-1}$  for  $\kappa \geq 1$ . Therefore

$$\|\Gamma_t(x, x)\| \leq \eta \max\{\kappa, 1\} \varphi(x)^\top (v_t + \eta I)^{-1} \varphi(x).$$

A simple application of Lemma 4 for  $n = 1$  and  $\Gamma(\cdot, \cdot) = k(\cdot, \cdot)$  now yields

$$\begin{aligned} \sum_{t=1}^T \|\Gamma_t(x, x)\| &\leq \eta \max\{\kappa, 1\} \sum_{t=1}^T \varphi(x_t)^\top (v_t + \eta I)^{-1} \varphi(x_t) \\ &= \eta \max\{\kappa, 1\} \log \det (I_T + \eta^{-1} K_T) \leq 2\eta \max\{\kappa, 1\} \gamma_T(k, \eta), \end{aligned}$$

which completes the proof.

#### C.4 Inter-task structure in regret for sum of separable kernels

We now present a generalization of Lemma 1 for multi-task kernels of the form  $\Gamma(x, x') = \sum_{j=1}^M k_j(x, x') B_j$ . This class of kernels is called the sum of separable (SoS) kernel and includes the diagonal kernel  $\Gamma(x, x') = \text{diag}(k_1(x, x'), \dots, k_n(x, x'))$  as a special case.

**Lemma 6 (Inter-task structure in regret for SoS kernel)** *Let  $\Gamma(x, x') = \sum_{j=1}^M k_j(x, x') B_j$  and  $B_j \in \mathbb{R}^{n \times n}$  be positive semi-definite. Then the following holds:*

$$\begin{aligned} \gamma_{nT}(\Gamma, \eta) &\leq \sum_{j=1}^M \rho_{B_j} \max\{\xi_{B_j}, 1\} \gamma_T(k_j, \eta), \\ \sum_{t=1}^T \|\Gamma_t(x_t, x_t)\| &\leq 2\eta \sum_{j=1}^M \max\{\xi_{B_j}, 1\} \gamma_T(k_j, \eta), \end{aligned}$$

where  $\rho_{B_j}$  and  $\xi_{B_j}$  denote the rank and the maximum eigenvalue of  $B_j$ , respectively and  $\gamma_T(k_j)$  is the maximum information gain corresponding to scalar kernel  $k_j$ . Moreover, if  $\Gamma(x, x') = \text{diag}(k_1(x, x'), \dots, k_n(x, x'))$  and each  $k_j$  is a stationary kernel, then

$$\gamma_{nT}(\Gamma, \eta) \leq \sum_{j=1}^n \gamma_T(k_j, \eta), \quad \sum_{t=1}^T \|\Gamma_t(x_t, x_t)\| \leq 2\eta \max_{1 \leq j \leq n} \gamma_T(k_j, \eta).$$

**Proof** We let, for each scalar kernel  $k_j$ , a feature map  $\varphi_j : \mathcal{X} \rightarrow \ell^2$ , so that  $k_j(x, x') = \varphi_j(x)^\top \varphi_j(x')$ . We now define the feature map  $\Phi : \mathcal{X} \rightarrow \mathcal{L}(\mathbb{R}^n, \ell^2)$  of the multi-task kernel  $\Gamma(x, x') = \sum_{j=1}^M k_j(x, x') B_j$  by

$$\Phi(x)y := \left( \varphi_1(x) \otimes B_1^{1/2}y, \dots, \varphi_M(x) \otimes B_M^{1/2}y \right), \quad \forall x \in \mathcal{X}, y \in \mathbb{R}^n,$$

with the inner product

$$\Phi(x)^\top \Phi(x') := \sum_{j=1}^M \left( \varphi_j(x) \otimes B_j^{1/2} \right)^\top \left( \varphi_j(x') \otimes B_j^{1/2} \right) = \sum_{j=1}^M \varphi_j(x)^\top \varphi_j(x') \cdot B_j.$$

We then have

$$V_t := \sum_{s=1}^t \Phi(x_s) \Phi(x_s)^\top = \sum_{s=1}^t \sum_{j=1}^M \varphi_j(x_s) \varphi_j(x_s)^\top \otimes B_j = \sum_{j=1}^M v_{t,j} \otimes B_j,$$

where  $v_{t,j} := \sum_{s=1}^t \varphi_j(x_s) \varphi_j(x_s)^\top$ . We further obtain from (10) that

$$\Gamma_t(x, x) = \sum_{j=1}^M \eta \left( \varphi_j(x) \otimes B_j^{1/2} \right)^\top \left( \sum_{j=1}^M v_{t,j} \otimes B_j + \eta I \right)^{-1} \left( \varphi_j(x) \otimes B_j^{1/2} \right).$$

Now each  $B_j$  is a positive semi-definite matrix and so is  $v_{t,j} \otimes B_j$ . Hence, for for all

$j \in [M]$ ,  $\left( \sum_{j=1}^M v_{t,j} \otimes B_j + \eta I \right)^{-1} \preceq (v_{t,j} \otimes B_j + \eta I)^{-1}$ . Therefore

$$\Gamma_t(x, x) \preceq \sum_{j=1}^M \eta \left( \varphi_j(x) \otimes B_j^{1/2} \right)^\top (v_{t,j} \otimes B_j + \eta I)^{-1} \left( \varphi_j(x) \otimes B_j^{1/2} \right) = \sum_{j=1}^M \Gamma_{t,j}(x, x), \quad (15)$$

where  $\Gamma_{t,j}(x, x) := \eta \left( \varphi_j(x) \otimes B_j^{1/2} \right)^\top (v_{t,j} \otimes B_j + \eta I)^{-1} \left( \varphi_j(x) \otimes B_j^{1/2} \right)$ . Now, let  $(\xi_{j,i}, u_{j,i})$  denotes the  $i$ -th eigenpair of  $B_j$ . A similar argument as in (4) then yields

$$(v_{t,j} \otimes B_j + \eta I)^{-1} = \sum_{i=1}^n (\xi_{j,i} v_{t,j} + \eta I)^{-1} \otimes u_{j,i} u_{j,i}^\top.$$



We then have from the mixed product property of Kronecker product and the orthonormality of  $\{u_{j,i}\}_{i=1}^n$  that

$$\begin{aligned}\Gamma_{t,j}(x, x) &= \sum_{i=1}^n \eta \xi_{j,i} \varphi_j(x)^\top (\xi_{j,i} v_{t,j} + \eta I)^{-1} \varphi_j(x) \cdot u_{j,i} u_{j,i}^\top \\ &= \sum_{i=1}^n \eta \varphi_j(x)^\top \left( v_{t,j} + \frac{\eta}{\xi_{j,i}} I \right)^{-1} \varphi_j(x) \cdot u_{j,i} u_{j,i}^\top.\end{aligned}$$

Since  $\left( v_{t,j} + \frac{\eta}{\xi_{j,i}} I \right)^{-1} \preceq (v_{t,j} + \eta I)^{-1}$  for  $\xi_{j,i} \leq 1$  and  $\left( v_{t,j} + \frac{\eta}{\xi_{j,i}} I \right)^{-1} \preceq \xi_{j,i} (v_{t,j} + \eta I)^{-1}$  for  $\xi_{j,i} \geq 1$ , we now have

$$\begin{aligned}\text{trace}(\Gamma_{t,j}(x, x)) &\leq \eta \sum_{i \in [n]: \xi_{j,i} > 0} \max\{\xi_{j,i}, 1\} \varphi_j(x)^\top (v_{t,j} + \eta I)^{-1} \varphi_j(x) \\ &\leq \eta \rho_{B_j} \max\{\xi_{B_j}, 1\} \varphi_j(x)^\top (v_{t,j} + \eta I)^{-1} \varphi_j(x).\end{aligned}$$

Similarly

$$\begin{aligned}\|\Gamma_{t,j}(x, x)\| &\leq \eta \max_{1 \leq i \leq n} \max\{\xi_{j,i}, 1\} \varphi_j(x)^\top (v_{t,j} + \eta I)^{-1} \varphi_j(x) \\ &\leq \eta \max\{\xi_{B_j}, 1\} \varphi_j(x)^\top (v_{t,j} + \eta I)^{-1} \varphi_j(x).\end{aligned}$$

Let  $K_{T,j} = [k_j(x_p, x_q)]_{p,q=1}^T$  denotes the kernel matrix corresponding to the scalar kernel  $k_j$ . An application of Lemma 4 for  $n = 1$  and  $\Gamma(\cdot, \cdot) = k_j(\cdot, \cdot)$  now yields

$$\begin{aligned}\sum_{t=1}^T \text{trace}(\Gamma_{t,j}(x_t, x_t)) &\leq \eta \rho_{B_j} \max\{\xi_{B_j}, 1\} \log \det(I_T + \eta^{-1} K_{T,j}) \quad \text{and} \\ \sum_{t=1}^T \|\Gamma_{t,j}(x_t, x_t)\| &\leq \eta \max\{\xi_{B_j}, 1\} \log \det(I_T + \eta^{-1} K_{T,j}).\end{aligned}$$

We then have from (15) and Lemma 4 that

$$\begin{aligned}\log \det(I_{nT} + \eta^{-1} G_T) &= \frac{1}{\eta} \sum_{t=1}^T \text{trace}(\Gamma_t(x_t, x_t)) \\ &\leq \frac{1}{\eta} \sum_{j=1}^M \sum_{t=1}^T \text{trace}(\Gamma_{t,j}(x_t, x_t)) \\ &\leq \sum_{j=1}^M \rho_{B_j} \max\{\xi_{B_j}, 1\} \log \det(I_T + \eta^{-1} K_{T,j}).\end{aligned}$$

Taking supremum over all possible subsets  $\mathcal{X}_T$  of  $\mathcal{X}$ , we now obtain that  $\gamma_{nT}(\Gamma, \eta) \leq \sum_{j=1}^M \rho_{B_j} \max\{\xi_{B_j}, 1\} \gamma_T(k_j, \eta)$ . We further have from (15) that

$$\sum_{t=1}^T \|\Gamma_t(x_t, x_t)\| \leq \sum_{j=1}^M \sum_{t=1}^T \|\Gamma_{t,j}(x_t, x_t)\| \leq 2\eta \sum_{j=1}^M \max\{\xi_{B_j}, 1\} \gamma_T(k_j, \eta),$$

which completes the proof for the first part.

For the diagonal kernel,  $M = n$  and each  $B_j$  is a diagonal matrix with 1 in the  $j$ -th diagonal entry and 0 in all others. In this case, we have

$$\Gamma_t(x, x) = \eta \sum_{j=1}^n \varphi_j(x)^\top (v_{t,j} + \eta I)^{-1} \varphi_j(x) \cdot B_j.$$

We then have from Lemma 4 that

$$\begin{aligned} \log \det (I_{nT} + \eta^{-1} G_T) &= \frac{1}{\eta} \sum_{t=1}^T \text{trace} (\Gamma_t(x_t, x_t)) \\ &= \sum_{t=1}^T \sum_{j=1}^n \varphi_j(x_t)^\top (v_{t,j} + \eta I)^{-1} \varphi_j(x_t) \cdot \text{trace} (B_j) \\ &= \sum_{j=1}^n \sum_{t=1}^T \varphi_j(x_t)^\top (v_{t,j} + \eta I)^{-1} \varphi_j(x_t) \\ &= \sum_{j=1}^n \log \det (I_T + \eta^{-1} K_{T,j}). \end{aligned}$$

Taking supremum over all possible subsets  $\mathcal{X}_T$  of  $\mathcal{X}$ , we now obtain that  $\gamma_{nT}(\Gamma, \eta) \leq \sum_{j=1}^n \gamma_T(k_j, \eta)$ . We further have

$$\|\Gamma_t(x, x)\| = \max_{1 \leq j \leq n} \eta \varphi_j(x)^\top (v_{t,j} + \eta I)^{-1} \varphi_j(x).$$

Let  $j^*(x) = \arg\max_{1 \leq j \leq n} k_j(x, x)$ . Since each  $k_j$  is stationary, i.e.,  $k_j(x, x') = k_j(x' - x)$ , we have  $j^*(x)$  is independent of  $x$ . We now let  $j^* = j^*(x)$  for all  $x$ . Then it can be easily checked that

$$\|\Gamma_t(x, x)\| = \eta \varphi_{j^*}(x)^\top (v_{t,j^*} + \eta I)^{-1} \varphi_{j^*}(x).$$

We now obtain from Lemma 4 that

$$\begin{aligned} \sum_{t=1}^T \|\Gamma_t(x_t, x_t)\| &= \eta \sum_{t=1}^T \varphi_{j^*}(x_t)^\top (v_{t,j^*} + \eta I)^{-1} \varphi_{j^*}(x_t) \\ &= \eta \log \det (I_T + \eta^{-1} K_{T,j^*}) \leq 2\eta \max_{1 \leq j \leq n} \gamma_T(k_j, \eta), \end{aligned}$$

which completes the proof for the second part.  $\blacksquare$

## D Analysis of MT-BKB

**Trading-off approximation accuracy and size** Given a dictionary  $\mathcal{D}_t = \{x_{i_1}, \dots, x_{i_{m_t}}\}$ , we define a map  $\Phi_{\mathcal{D}_t} : \ell^2 \rightarrow \mathbb{R}^{nm_t}$  by

$$\Phi_{\mathcal{D}_t} \theta := \left[ \frac{1}{\sqrt{p_{t,i_1}}} (\Phi(x_{i_1})^\top \theta)^\top, \dots, \frac{1}{\sqrt{p_{t,i_{m_t}}}} (\Phi(x_{i_{m_t}})^\top \theta)^\top \right]^\top, \quad \forall \theta \in \ell^2, \quad (16)$$

where  $p_{t,i_j} = \min \left\{ q \left\| \tilde{\Gamma}_{t-1}(x_{i_j}, x_{i_j}) \right\|, 1 \right\}$  for all  $j \in [m_t]$ .

**Lemma 7 (Approximation properties)** *For any  $T \geq 1$ ,  $\varepsilon \in (0, 1)$  and  $\delta \in (0, 1]$ , set  $\rho = \frac{1+\varepsilon}{1-\varepsilon}$  and  $q = \frac{6\rho \ln(2T/\delta)}{\varepsilon^2}$ . Then, for any  $\eta > 0$ , with probability at least  $1 - \delta$ , the following hold uniformly over all  $t \in [T]$  :*

$$\begin{aligned} (1 - \varepsilon)\Phi_{\mathcal{X}_t}^\top \Phi_{\mathcal{X}_t} - \varepsilon\eta I &\preceq \Phi_{\mathcal{D}_t}^\top \Phi_{\mathcal{D}_t} \preceq (1 + \varepsilon)\Phi_{\mathcal{X}_t}^\top \Phi_{\mathcal{X}_t} + \varepsilon\eta I, \\ m_t &\leq 6\rho q (1 + \kappa/\eta) \sum_{s=1}^t \|\Gamma_s(x_s, x_s)\|. \end{aligned}$$

**Proof** Let  $S_t$  be an  $nt$ -by- $nt$  block diagonal matrix with  $i$ -th diagonal block  $[S_t]_i = \frac{1}{\sqrt{p_{t,i}}}I_n$  if  $x_i \in \mathcal{D}_t$ , and  $[S_t]_i = 0$  if  $x_i \notin \mathcal{D}_t$ ,  $1 \leq i \leq t$ . We then have  $\Phi_{\mathcal{D}_t}^\top \Phi_{\mathcal{D}_t} = \Phi_{\mathcal{X}_t}^\top S_t^\top S_t \Phi_{\mathcal{X}_t}$ . The proof now can be completed by following Calandriello et al. (2019, Theorem 1).  $\blacksquare$

**Remark 4** *Note that although tuning the approximation trade-off parameter  $q$  requires the knowledge of the time horizon  $T$  in advance, Lemma 7 is quite robust to the uncertainty on  $T$ . If the horizon is not known, then after the  $T$ -th step, one can increase  $q$  according to the new desired horizon, and update the dictionary with this new value of  $q$ . Combining this with a standard doubling trick preserve the approximation properties (Calandriello et al., 2019).*

**Approximating the confidence set** We now focus on the dictionary  $\mathcal{D}_t$  chosen by MT-BKB at each step and discuss a principled approach to compute the approximations  $\tilde{\mu}_t(x)$  and  $\tilde{\Gamma}_t(x, x)$ . To this end, we let

$$P_t = \Phi_{\mathcal{D}_t}^\top (\Phi_{\mathcal{D}_t} \Phi_{\mathcal{D}_t}^\top)^+ \Phi_{\mathcal{D}_t} \quad (17)$$

denote the symmetric orthogonal projection operator on the subspace of  $\mathcal{L}(\mathbb{R}^n, \ell^2)$  that is spanned by  $\Phi(x_{i_1}), \dots, \Phi(x_{i_{m_t}})$ . We also let  $\hat{\Phi}_t(x) = P_t \Phi(x)$  denote the projection of  $\Phi(x)$ . We now define a map  $\hat{\Phi}_{\mathcal{X}_t} : \ell^2 \rightarrow \mathbb{R}^{nt}$  by

$$\hat{\Phi}_{\mathcal{X}_t} \theta := \left[ \left( \hat{\Phi}_t(x_1)^\top \theta \right)^\top, \dots, \left( \hat{\Phi}_t(x_t)^\top \theta \right)^\top \right]^\top, \quad \forall \theta \in \ell^2.$$

We then have  $\hat{\Phi}_{\mathcal{X}_t} = \Phi_{\mathcal{X}_t} P_t$  and  $\hat{\Phi}_{\mathcal{X}_t} \hat{\Phi}_{\mathcal{X}_t}^\top = \Phi_{\mathcal{X}_t} P_t \Phi_{\mathcal{X}_t}^\top$ .

**Lemma 8 (Approximation as given by projection)** *Let  $\hat{V}_t := \hat{\Phi}_{\mathcal{X}_t}^\top \hat{\Phi}_{\mathcal{X}_t}$ . Then, for any  $\eta > 0$  and  $t \geq 1$ , the following holds:*

$$\begin{aligned} \tilde{\mu}_t(x) &= \Phi(x)^\top \left( \hat{V}_t + \eta I \right)^{-1} \sum_{s=1}^t \hat{\Phi}_t(x_s) y_s, \\ \tilde{\Gamma}_t(x, x) &= \eta \Phi(x)^\top \left( \hat{V}_t + \eta I \right)^{-1} \Phi(x). \end{aligned}$$

**Proof** We first note that

$$\tilde{\Phi}_t(x)^\top \tilde{\Phi}_t(x') = \tilde{G}_t(x)^\top \tilde{G}_t^+ \tilde{G}_t(x') = \Phi(x)^\top P_t \Phi(x').$$

We now define an  $nt \times nm_t$  matrix  $\tilde{\Phi}_{\mathcal{X}_t} = [\tilde{\Phi}_t(x_1), \dots, \tilde{\Phi}_t(x_t)]^\top$ . We then have

$$\tilde{\Phi}_{\mathcal{X}_t} \tilde{\Phi}_t(x) = \Phi_{\mathcal{X}_t} P_t \Phi(x) = \hat{\Phi}_{\mathcal{X}_t} \Phi(x), \quad \tilde{\Phi}_{\mathcal{X}_t} \tilde{\Phi}_{\mathcal{X}_t}^\top = \Phi_{\mathcal{X}_t} P_t \Phi_{\mathcal{X}_t}^\top = \hat{\Phi}_{\mathcal{X}_t} \hat{\Phi}_{\mathcal{X}_t}^\top, \quad (18)$$

where  $P_t$  is the projection operator as defined in (17). We also have  $\tilde{V}_t := \sum_{s=1}^t \tilde{\Phi}_t(x_s) \tilde{\Phi}_t(x_s)^\top = \tilde{\Phi}_{\mathcal{X}_t}^\top \tilde{\Phi}_{\mathcal{X}_t}$ . Therefore

$$\begin{aligned} \tilde{\mu}_t(x) &= \tilde{\Phi}_t(x)^\top (\tilde{\Phi}_{\mathcal{X}_t}^\top \tilde{\Phi}_{\mathcal{X}_t} + \eta I_{nm_t})^{-1} \sum_{s=1}^t \tilde{\Phi}_t(x_s) y_s \\ &= \tilde{\Phi}_t(x)^\top (\tilde{\Phi}_{\mathcal{X}_t}^\top \tilde{\Phi}_{\mathcal{X}_t} + \eta I_{nm_t})^{-1} \tilde{\Phi}_{\mathcal{X}_t}^\top Y_t \\ &= \tilde{\Phi}_t(x)^\top \tilde{\Phi}_{\mathcal{X}_t}^\top (\tilde{\Phi}_{\mathcal{X}_t} \tilde{\Phi}_{\mathcal{X}_t}^\top + \eta I_{nt})^{-1} Y_t \\ &= \Phi(x)^\top \hat{\Phi}_{\mathcal{X}_t}^\top (\hat{\Phi}_{\mathcal{X}_t} \hat{\Phi}_{\mathcal{X}_t}^\top + \eta I_{nt})^{-1} Y_t \\ &= \Phi(x)^\top (\hat{\Phi}_{\mathcal{X}_t}^\top \hat{\Phi}_{\mathcal{X}_t} + \eta I)^{-1} \hat{\Phi}_{\mathcal{X}_t}^\top Y_t = \Phi(x)^\top (\hat{V}_t + \eta I)^{-1} \sum_{s=1}^t \hat{\Phi}_t(x_s) y_s, \end{aligned}$$

where in third and fifth step, we have used Lemma 2, and in fourth step, we have used (18). Further

$$\begin{aligned} \tilde{\Gamma}_t(x, x) &= \Gamma(x, x) - \tilde{\Phi}_t(x)^\top \tilde{\Phi}_t(x) + \eta \tilde{\Phi}_t(x)^\top (\tilde{\Phi}_{\mathcal{X}_t}^\top \tilde{\Phi}_{\mathcal{X}_t} + \eta I_{nm_t})^{-1} \tilde{\Phi}_t(x) \\ &= \Gamma(x, x) - \tilde{\Phi}_t(x)^\top \left( I_{nm_t} - \eta (\tilde{\Phi}_{\mathcal{X}_t}^\top \tilde{\Phi}_{\mathcal{X}_t} + \eta I_{nm_t})^{-1} \right) \tilde{\Phi}_t(x) \\ &= \Gamma(x, x) - \tilde{\Phi}_t(x)^\top \tilde{\Phi}_{\mathcal{X}_t}^\top (\tilde{\Phi}_{\mathcal{X}_t} \tilde{\Phi}_{\mathcal{X}_t}^\top + \eta I_{nt})^{-1} \tilde{\Phi}_{\mathcal{X}_t} \tilde{\Phi}_t(x) \\ &= \Phi(x)^\top \Phi(x) - \Phi(x)^\top \hat{\Phi}_{\mathcal{X}_t}^\top (\hat{\Phi}_{\mathcal{X}_t} \hat{\Phi}_{\mathcal{X}_t}^\top + \eta I_{nt})^{-1} \hat{\Phi}_{\mathcal{X}_t} \Phi(x) \\ &= \Phi(x)^\top \left( I - \hat{\Phi}_{\mathcal{X}_t}^\top (\hat{\Phi}_{\mathcal{X}_t} \hat{\Phi}_{\mathcal{X}_t}^\top + \eta I_{nt})^{-1} \hat{\Phi}_{\mathcal{X}_t} \right) \Phi(x) \\ &= \eta \Phi(x)^\top (\hat{\Phi}_{\mathcal{X}_t}^\top \hat{\Phi}_{\mathcal{X}_t} + \eta I)^{-1} \Phi(x) = \eta \Phi(x)^\top (\hat{V}_t + \eta I)^{-1} \Phi(x), \end{aligned}$$

where in third and sixth step, we have used Lemma 2, and in fourth step, we have used (18).  $\blacksquare$

**Lemma 9 (Multi-task concentration under Nyström approximation)** *Let  $f \in \mathcal{H}_\Gamma(\mathcal{X})$  and the noise vectors  $\{\varepsilon_t\}_{t \geq 1}$  be  $\sigma$ -sub-Gaussian. Further, for any  $\eta > 0$ ,  $\varepsilon \in (0, 1)$  and  $t \geq 1$ , let  $(1 - \varepsilon) \Phi_{\mathcal{X}_t}^\top \Phi_{\mathcal{X}_t} - \varepsilon \eta I \preceq \Phi_{\mathcal{D}_t}^\top \Phi_{\mathcal{D}_t} \preceq (1 + \varepsilon) \Phi_{\mathcal{X}_t}^\top \Phi_{\mathcal{X}_t} + \varepsilon \eta I$ . Then, for any  $\delta \in (0, 1]$ , with probability at least  $1 - \delta$ , the following holds uniformly over all  $x \in \mathcal{X}$  and  $t \geq 1$ :*

$$\|f(x) - \tilde{\mu}_t(x)\|_2 \leq \left( c_\varepsilon \|f\|_\Gamma + \frac{\sigma}{\sqrt{\eta}} \sqrt{2 \log(1/\delta) + \log \det(I_{nt} + \eta^{-1} G_t)} \right) \|\tilde{\Gamma}_t(x, x)\|^{1/2},$$

where  $c_\varepsilon = 1 + \frac{1}{\sqrt{1-\varepsilon}}$ .

**Proof** Let us first define  $\tilde{\alpha}_t(x) := \Phi(x)^\top \left( \hat{V}_t + \eta I \right)^{-1} \sum_{s=1}^t \hat{\Phi}_t(x_s) f(x_s)$ , where

$\hat{V}_t = \hat{\Phi}_{\mathcal{X}_t}^\top \hat{\Phi}_{\mathcal{X}_t}$ . We now note that  $f(x) = \Phi(x)^\top \theta^*$  and  $\tilde{\alpha}_t(x) = \Phi(x)^\top \left( \hat{V}_t + \eta I \right)^{-1} \hat{\Phi}_{\mathcal{X}_t}^\top \Phi_{\mathcal{X}_t} \theta^*$  for some  $\theta^* \in \ell^2$ , so that  $\|f\|_\Gamma = \|\theta^*\|_2$ . We then have

$$\begin{aligned}
\|f(x) - \tilde{\alpha}_t(x)\|_2 &= \left\| \Phi(x)^\top \left( \theta^* - \left( \hat{V}_t + \eta I \right)^{-1} \hat{\Phi}_{\mathcal{X}_t}^\top \Phi_{\mathcal{X}_t} \theta^* \right) \right\|_2 \\
&\leq \left\| \Phi(x)^\top \left( \hat{V}_t + \eta I \right)^{-1/2} \right\| \left\| \theta^* - \left( \hat{V}_t + \eta I \right)^{-1} \hat{\Phi}_{\mathcal{X}_t}^\top \Phi_{\mathcal{X}_t} \theta^* \right\|_{(\hat{V}_t + \eta I)} \\
&= \left\| \Phi(x)^\top \left( \hat{V}_t + \eta I \right)^{-1} \Phi(x) \right\|^{1/2} \left\| \left( \hat{V}_t + \eta I \right) \theta^* - \hat{\Phi}_{\mathcal{X}_t}^\top \Phi_{\mathcal{X}_t} \theta^* \right\|_{(\hat{V}_t + \eta I)^{-1}} \\
&= \eta^{-1/2} \left\| \tilde{\Gamma}_t(x, x) \right\|^{1/2} \left\| \eta \theta^* - \hat{\Phi}_{\mathcal{X}_t}^\top \left( \Phi_{\mathcal{X}_t} - \hat{\Phi}_{\mathcal{X}_t} \right) \theta^* \right\|_{(\hat{V}_t + \eta I)^{-1}} \\
&\leq \eta^{-1/2} \left\| \tilde{\Gamma}_t(x, x) \right\|^{1/2} \left( \eta \|\theta^*\|_{(\hat{V}_t + \eta I)^{-1}} + \left\| \hat{\Phi}_{\mathcal{X}_t}^\top \Phi_{\mathcal{X}_t} (I - P_t) \theta^* \right\|_{(\hat{V}_t + \eta I)^{-1}} \right) \\
&\leq \left( \|\theta^*\|_2 + \eta^{-1/2} \left\| \left( \hat{V}_t + \eta I \right)^{-1/2} \hat{\Phi}_{\mathcal{X}_t}^\top \Phi_{\mathcal{X}_t} (I - P_t) \theta^* \right\|_2 \right) \left\| \tilde{\Gamma}_t(x, x) \right\|^{1/2}.
\end{aligned}$$

Here in the fourth step, we have used Lemma 8 and in the second last step, we have used  $\hat{\Phi}_{\mathcal{X}_t} = \Phi_{\mathcal{X}_t} P_t$ , where  $P_t$  is the projection operator as defined in (17). The last step is controlled as  $\|\theta^*\|_{(\hat{V}_t + \eta I)^{-1}} \leq \eta^{-1/2} \|\theta^*\|_2$ . We now have

$$\begin{aligned}
\left\| \left( \hat{V}_t + \eta I \right)^{-1/2} \hat{\Phi}_{\mathcal{X}_t}^\top \Phi_{\mathcal{X}_t} (I - P_t) \theta^* \right\|_2 &\leq \left\| \left( \hat{V}_t + \eta I \right)^{-1/2} \hat{\Phi}_{\mathcal{X}_t}^\top \right\| \left\| \Phi_{\mathcal{X}_t} (I - P_t) \right\| \|\theta^*\|_2 \\
&\leq \left\| \Phi_{\mathcal{X}_t} (I - P_t) \Phi_{\mathcal{X}_t}^\top \right\|^{1/2} \|\theta^*\|_2,
\end{aligned}$$

where we have used that  $\left\| \left( \hat{V}_t + \eta I \right)^{-1/2} \hat{\Phi}_{\mathcal{X}_t}^\top \right\| = \left\| \hat{\Phi}_{\mathcal{X}_t} (\hat{\Phi}_{\mathcal{X}_t}^\top \hat{\Phi}_{\mathcal{X}_t} + \eta I)^{-1} \hat{\Phi}_{\mathcal{X}_t}^\top \right\|^{1/2} \leq 1$  and  $(I - P_t)^2 = I - P_t$ . We now observe from Lemma 2 and our hypothesis  $(1 - \varepsilon) \Phi_{\mathcal{X}_t}^\top \Phi_{\mathcal{X}_t} - \varepsilon \eta I \preceq \Phi_{\mathcal{D}_t}^\top \Phi_{\mathcal{D}_t} \preceq (1 + \varepsilon) \Phi_{\mathcal{X}_t}^\top \Phi_{\mathcal{X}_t} + \varepsilon \eta I$  that

$$I - P_t \preceq I - \Phi_{\mathcal{D}_t}^\top (\Phi_{\mathcal{D}_t} \Phi_{\mathcal{D}_t}^\top + \eta I_{nm_t})^{-1} \Phi_{\mathcal{D}_t} = \eta (\Phi_{\mathcal{D}_t}^\top \Phi_{\mathcal{D}_t} + \eta I)^{-1} \preceq \frac{\eta}{1 - \varepsilon} (\Phi_{\mathcal{X}_t}^\top \Phi_{\mathcal{X}_t} + \eta I)^{-1},$$

and therefore,  $\left\| \Phi_{\mathcal{X}_t} (I - P_t) \Phi_{\mathcal{X}_t}^\top \right\|^{1/2} \leq \sqrt{\frac{\eta}{1 - \varepsilon}} \left\| \Phi_{\mathcal{X}_t} (\Phi_{\mathcal{X}_t}^\top \Phi_{\mathcal{X}_t} + \eta I)^{-1} \Phi_{\mathcal{X}_t}^\top \right\|^{1/2} \leq \sqrt{\frac{\eta}{1 - \varepsilon}}$ . Putting it all together, we now have

$$\|f(x) - \tilde{\alpha}_t(x)\|_2 \leq \|\theta^*\|_2 \left( 1 + \frac{1}{\sqrt{1 - \varepsilon}} \right) \left\| \tilde{\Gamma}_t(x, x) \right\|^{1/2} = c_\varepsilon \|f\|_\Gamma \left\| \tilde{\Gamma}_t(x, x) \right\|^{1/2}, \quad (19)$$

where we have used that  $\|\theta^*\|_2 = \|f\|_\Gamma$  and  $c_\varepsilon = 1 + \frac{1}{\sqrt{1 - \varepsilon}}$ . We further obtain from

Lemma 8 that

$$\begin{aligned}
\|\tilde{\mu}_t(x) - \tilde{\alpha}_t(x)\|_2 &= \left\| \Phi(x)^\top \left( \hat{V}_t + \eta I \right)^{-1} \sum_{s=1}^t \hat{\Phi}_t(x_s) (y_s - f(x_s)) \right\|_2 \\
&\leq \left\| \Phi(x)^\top \left( \hat{V}_t + \eta I \right)^{-1/2} \right\| \left\| \sum_{s=1}^t \hat{\Phi}_t(x_s) \varepsilon_s \right\|_{(\hat{V}_t + \eta I)^{-1}} \\
&= \left\| \Phi(x)^\top \left( \hat{V}_t + \eta I \right)^{-1} \Phi(x) \right\|^{1/2} \left\| \hat{\Phi}_{\mathcal{X}_t}^\top E_t \right\|_{(\hat{V}_t + \eta I)^{-1}} \\
&= \eta^{-1/2} \left\| \tilde{\Gamma}_t(x, x) \right\|^{1/2} \left\| \hat{\Phi}_{\mathcal{X}_t}^\top E_t \right\|_{(\hat{V}_t + \eta I)^{-1}},
\end{aligned}$$

where  $E_t = [\varepsilon_1^\top, \dots, \varepsilon_t^\top]^\top$  denotes an  $nt \times 1$  vector formed by concatenating the noise vectors  $\varepsilon_i$ ,  $1 \leq i \leq t$ . We now have

$$\begin{aligned}
\left\| \hat{\Phi}_{\mathcal{X}_t}^\top E_t \right\|_{(\hat{V}_t + \eta I)^{-1}}^2 &= E_t^\top \hat{\Phi}_{\mathcal{X}_t} \left( \hat{\Phi}_{\mathcal{X}_t}^\top \hat{\Phi}_{\mathcal{X}_t} + \eta I \right)^{-1} \hat{\Phi}_{\mathcal{X}_t}^\top E_t \\
&= E_t^\top \left( I_{nt} - \eta \left( \hat{\Phi}_{\mathcal{X}_t} \hat{\Phi}_{\mathcal{X}_t}^\top + \eta I_{nt} \right)^{-1} \right) E_t \\
&\leq E_t^\top \left( I_{nt} - \eta \left( \Phi_{\mathcal{X}_t} \Phi_{\mathcal{X}_t}^\top + \eta I_{nt} \right)^{-1} \right) E_t \\
&= E_t^\top \Phi_{\mathcal{X}_t} \left( \Phi_{\mathcal{X}_t}^\top \Phi_{\mathcal{X}_t} + \eta I \right)^{-1} \Phi_{\mathcal{X}_t}^\top E_t = \left\| \Phi_{\mathcal{X}_t}^\top E_t \right\|_{(V_t + \eta I)^{-1}}^2,
\end{aligned}$$

where in second and fourth step, we have used Lemma 2, and in third step, we have used  $\hat{\Phi}_{\mathcal{X}_t} \hat{\Phi}_{\mathcal{X}_t}^\top = \Phi_{\mathcal{X}_t} P_t \Phi_{\mathcal{X}_t}^\top \preceq \Phi_{\mathcal{X}_t} \Phi_{\mathcal{X}_t}^\top$ . We then have

$$\begin{aligned}
\|\tilde{\mu}_t(x) - \tilde{\alpha}_t(x)\|_2 &\leq \eta^{-1/2} \left\| \sum_{s=1}^t \Phi(x_s) \varepsilon_s \right\|_{(V_t + \eta I)^{-1}} \left\| \tilde{\Gamma}_t(x, x) \right\|^{1/2} \\
&= \eta^{-1/2} \|S_t\|_{(V_t + \eta I)^{-1}} \left\| \tilde{\Gamma}_t(x, x) \right\|^{1/2}, \tag{20}
\end{aligned}$$

where  $S_t := \sum_{s=1}^t \Phi(x_s) \varepsilon_s$ . Combining (19) and (20) together, we now obtain

$$\begin{aligned}
\|f(x) - \tilde{\mu}_t(x)\|_2 &\leq \|f(x) - \tilde{\alpha}_t(x)\|_2 + \|\tilde{\alpha}_t(x) - \tilde{\mu}_t(x)\|_2 \\
&\leq \left( c_\varepsilon \|f\|_\Gamma + \eta^{-1/2} \|S_t\|_{(V_t + \eta I)^{-1}} \right) \left\| \tilde{\Gamma}_t(x, x) \right\|^{1/2}.
\end{aligned}$$

We now conclude the proof using Lemma 3. ■

**Preventing variance starvation** We now show that an accurate dictionary helps us avoid variance starvation in Nyström approximation.

**Lemma 10 (Predictive variance control)** For any  $\eta > 0$  and  $\varepsilon \in (0, 1)$ , let  $\rho = (1 + \varepsilon)/(1 - \varepsilon)$  and  $(1 - \varepsilon)\Phi_{\mathcal{X}_t}^\top \Phi_{\mathcal{X}_t} - \varepsilon\eta I \preceq \Phi_{\mathcal{D}_t}^\top \Phi_{\mathcal{D}_t} \preceq (1 + \varepsilon)\Phi_{\mathcal{X}_t}^\top \Phi_{\mathcal{X}_t} + \varepsilon\eta I$ . Then

$$\frac{1}{\rho}\Gamma_t(x, x) \preceq \tilde{\Gamma}_t(x, x) \preceq \rho\Gamma_t(x, x).$$

**Proof** We first note that  $\hat{\Phi}_{\mathcal{X}_t}^\top \hat{\Phi}_{\mathcal{X}_t} = P_t \Phi_{\mathcal{X}_t}^\top \Phi_{\mathcal{X}_t} P_t$ , where  $P_t$  is the projection operator as defined in (17). Then our hypothesis  $(1 - \varepsilon)\Phi_{\mathcal{X}_t}^\top \Phi_{\mathcal{X}_t} - \varepsilon\eta I \preceq \Phi_{\mathcal{D}_t}^\top \Phi_{\mathcal{D}_t} \preceq (1 + \varepsilon)\Phi_{\mathcal{X}_t}^\top \Phi_{\mathcal{X}_t} + \varepsilon\eta I$  can be re-formulated as

$$\frac{1}{1 + \varepsilon} P_t \Phi_{\mathcal{D}_t}^\top \Phi_{\mathcal{D}_t} P_t - \frac{\varepsilon\eta}{1 + \varepsilon} P_t \preceq \hat{\Phi}_{\mathcal{X}_t}^\top \hat{\Phi}_{\mathcal{X}_t} \preceq \frac{1}{1 - \varepsilon} P_t \Phi_{\mathcal{D}_t}^\top \Phi_{\mathcal{D}_t} P_t + \frac{\varepsilon\eta}{1 - \varepsilon} P_t.$$

Since, by definition,  $P_t \Phi_{\mathcal{D}_t}^\top = \Phi_{\mathcal{D}_t}^\top$  and  $P_t \preceq I$ , we have

$$\frac{1}{1 + \varepsilon} \Phi_{\mathcal{D}_t}^\top \Phi_{\mathcal{D}_t} - \frac{\varepsilon\eta}{1 + \varepsilon} \preceq \hat{\Phi}_{\mathcal{X}_t}^\top \hat{\Phi}_{\mathcal{X}_t} \preceq \frac{1}{1 - \varepsilon} \Phi_{\mathcal{D}_t}^\top \Phi_{\mathcal{D}_t} + \frac{\varepsilon\eta}{1 - \varepsilon},$$

and, thus, in turn

$$\frac{1}{1 + \varepsilon} (\Phi_{\mathcal{D}_t}^\top \Phi_{\mathcal{D}_t} + \eta I) \preceq \hat{\Phi}_{\mathcal{X}_t}^\top \hat{\Phi}_{\mathcal{X}_t} + \eta I \preceq \frac{1}{1 - \varepsilon} (\Phi_{\mathcal{D}_t}^\top \Phi_{\mathcal{D}_t} + \eta I).$$

We now obtain from our hypothesis that

$$\frac{1 - \varepsilon}{1 + \varepsilon} (\Phi_{\mathcal{X}_t}^\top \Phi_{\mathcal{X}_t} + \eta I) \preceq \hat{\Phi}_{\mathcal{X}_t}^\top \hat{\Phi}_{\mathcal{X}_t} + \eta I \preceq \frac{1 + \varepsilon}{1 - \varepsilon} (\Phi_{\mathcal{X}_t}^\top \Phi_{\mathcal{X}_t} + \eta I).$$

This further implies that

$$\frac{1 - \varepsilon}{1 + \varepsilon} \Phi(x)^\top (V_t + \eta I)^{-1} \Phi(x) \preceq \Phi(x)^\top \left( \hat{V}_t + \eta I \right)^{-1} \Phi(x) \preceq \frac{1 + \varepsilon}{1 - \varepsilon} \Phi(x)^\top (V_t + \eta I)^{-1} \Phi(x),$$

which completes the proof.  $\blacksquare$

## D.1 Regret bound and dictionary size for MT-BKB (Proof of Theorem 3)

Since the scalarization functions  $s_\lambda$  is  $L_\lambda$ -Lipschitz in the  $\ell_2$  norm, we have

$$|s_{\lambda_t}(f(x)) - s_{\lambda_t}(\tilde{\mu}_{t-1}(x))| \leq L_{\lambda_t} \|f(x) - \tilde{\mu}_{t-1}(x)\|_2.$$

Since  $\tilde{\mu}_0(x) = 0$ ,  $\tilde{\Gamma}_0(x, x) = \Gamma(x, x)$  and  $\|f\|_\Gamma \leq b$ , we have

$$\|f(x) - \tilde{\mu}_0(x)\|_2 = \|\Gamma_x^\top f\|_2 \leq \|f\|_\Gamma \|\Gamma_x\| = \|f\|_\Gamma \|\Gamma_x^\top \Gamma_x\|^{1/2} \leq b \|\tilde{\Gamma}_0(x, x)\|^{1/2}.$$

Further, since  $\log(1 + ax) \leq a \log(1 + x)$  holds for any  $a \geq 1$  and  $x \geq 0$ , we obtain from Lemma 4 and Lemma 10 that

$$\begin{aligned} \log \det (I_{nt} + \eta^{-1} G_t) &= \sum_{s=1}^t \log \det (I_n + \eta^{-1} \Gamma_{s-1}(x_s, x_s)) \\ &\leq \rho \sum_{s=1}^t \log \det (I_n + \eta^{-1} \tilde{\Gamma}_{s-1}(x_s, x_s)), \end{aligned} \quad (21)$$

where  $\rho = \frac{1+\varepsilon}{1-\varepsilon}$ . Let us now assume, for any  $t \geq 1$ , that

$$(1 - \varepsilon) \Phi_{\mathcal{X}_t}^\top \Phi_{\mathcal{X}_t} - \varepsilon \eta I \preceq \Phi_{\mathcal{D}_t}^\top \Phi_{\mathcal{D}_t} \preceq (1 + \varepsilon) \Phi_{\mathcal{X}_t}^\top \Phi_{\mathcal{X}_t} + \varepsilon \eta I. \quad (22)$$

Then, from (21) and Lemma 9, the following holds with probability at least  $1 - \delta/2$ :

$$\forall t \geq 1, \forall x \in \mathcal{X}, \quad |s_{\lambda_t}(f(x)) - s_{\lambda_t}(\tilde{\mu}_{t-1}(x))| \leq L_{\lambda_t} \tilde{\beta}_{t-1} \left\| \tilde{\Gamma}_{t-1}(x, x) \right\|^{1/2}, \quad (23)$$

where  $\tilde{\beta}_t = c_\varepsilon b + \frac{\sigma}{\sqrt{\eta}} \sqrt{2 \log(2/\delta) + \rho \sum_{s=1}^t \log \det (I_n + \eta^{-1} \tilde{\Gamma}_{s-1}(x_s, x_s))}$ ,  $t \geq 0$  and  $c_\varepsilon = 1 + \frac{1}{\sqrt{1-\varepsilon}}$ . We can now upper bound the *instantaneous regret* at time  $t \geq 1$  as

$$\begin{aligned} r_{\lambda_t}(x_t) &:= s_{\lambda_t}(f(x_{\lambda_t}^*)) - s_{\lambda_t}(f(x_t)) \\ &\leq s_{\lambda_t}(\tilde{\mu}_{t-1}(x_{\lambda_t}^*)) + L_{\lambda_t} \tilde{\beta}_{t-1} \left\| \tilde{\Gamma}_{t-1}(x_{\lambda_t}^*, x_{\lambda_t}^*) \right\|^{1/2} - s_{\lambda_t}(f(x_t)) \\ &\leq s_{\lambda_t}(\tilde{\mu}_{t-1}(x_t)) + L_{\lambda_t} \tilde{\beta}_{t-1} \left\| \tilde{\Gamma}_{t-1}(x_t, x_t) \right\|^{1/2} - s_{\lambda_t}(f(x_t)) \\ &\leq 2L_{\lambda_t} \tilde{\beta}_{t-1} \left\| \tilde{\Gamma}_{t-1}(x_t, x_t) \right\|^{1/2}. \end{aligned}$$

Here in the first and third step, we have used (23). The second step follows from the choice of  $x_t$ . Since  $\tilde{\beta}_t$  is a monotonically increasing function in  $t$  and  $L_{\lambda_t} \leq L$  for all  $t$ , we now have

$$\begin{aligned} \sum_{t=1}^T r_{\lambda_t}(x_t) &\leq 2L \tilde{\beta}_T \sum_{t=1}^T \left\| \tilde{\Gamma}_{t-1}(x_t, x_t) \right\|^{1/2} \leq 2L \tilde{\beta}_T \sqrt{\rho T \sum_{t=1}^T \left\| \Gamma_{t-1}(x_t, x_t) \right\|} \\ &\leq 2L \tilde{\beta}_T \sqrt{\rho(1 + \kappa/\eta) T \sum_{t=1}^T \left\| \Gamma_t(x_t, x_t) \right\|}, \end{aligned}$$

where the second last step is due to the Cauchy-Schwartz inequality and Lemma 10, and the last step is due to Lemma 5. A similar argument as in (21) now yields

$$\begin{aligned} \sum_{t=1}^T \log \det (I_n + \eta^{-1} \tilde{\Gamma}_{t-1}(x_t, x_t)) &\leq \rho \sum_{t=1}^T \log \det (I_n + \eta^{-1} \Gamma_{t-1}(x_t, x_t)) \\ &= \rho \log \det (I_{nT} + \eta^{-1} G_T) \leq 2\rho \gamma_{nT}(\Gamma, \eta). \end{aligned}$$



We then have  $\tilde{\beta}_T \leq c_\varepsilon b + \frac{\sigma}{\sqrt{\eta}} \sqrt{2(\log(2/\delta) + \rho^2 \gamma_{nT}(\Gamma, \eta))}$ . Setting  $q = \frac{6\rho \ln(4T/\delta)}{\varepsilon^2}$ , we now have from Lemma 7, that with probability at least  $1 - \delta/2$ , uniformly across all  $t \in [T]$ , the dictionary size  $m_t \leq 6\rho q(1 + \kappa/\eta) \sum_{s=1}^t \|\Gamma_s(x_s, x_s)\|$  and (22) is true. Taking an expectation over  $\{\lambda_i\}_{i=1}^T \sim P_\lambda$  and using a union bound argument, we then obtain, with probability at least  $1 - \delta$ , the cumulative regret

$$R_C^{\text{MT-BKB}}(T) \leq 2L \left( c_\varepsilon b + \frac{\sigma}{\sqrt{\eta}} \sqrt{2(\log(1/\delta) + \rho^2 \gamma_{nT}(\Gamma, \eta))} \right) \sqrt{\rho(1 + \kappa/\eta) T \sum_{t=1}^T \|\Gamma_t(x_t, x_t)\|}.$$

We conclude the proof by noting that  $\rho = \frac{1+\varepsilon}{1-\varepsilon} > 1$  and  $c_\varepsilon = 1 + \frac{1}{\sqrt{1-\varepsilon}} \leq 2\rho$ .

## E Additional details on experiments

**Cumulative regret using linear scalarization** We sample from  $P_\lambda$  as  $\lambda = u/\|u\|_1$ , where  $u$  is uniformly sampled from  $[0, 1]^n$ . We plot the time-average cumulative regret  $\frac{1}{T} R_C(T)$  in Figure 2.

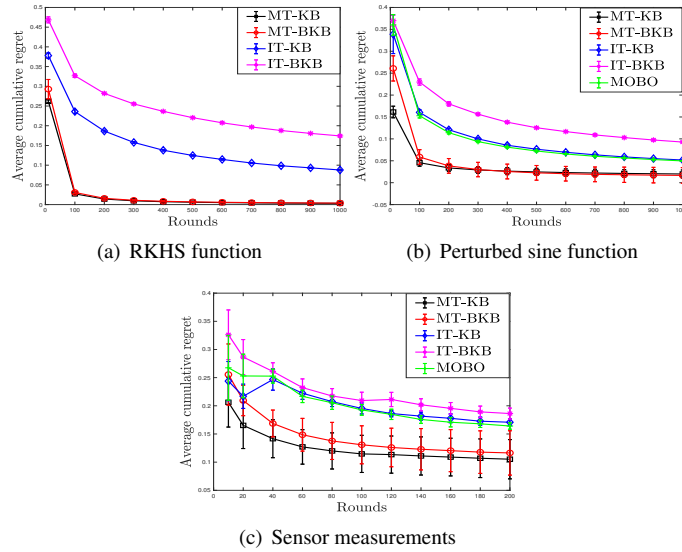


Figure 2: Comparison of time-average cumulative regret of MT-KB and MT-BKB with IT-KB, IT-BKB and MOBO using linear scalarization.

**Comparison of Bayes regret** We compare the Bayes regret  $R_B(T)$  of MT-KB and MT-BKB with independent task benchmarks IT-KB, IT-BKB and MOBO using Chebyshev scalarization in Figure 3.

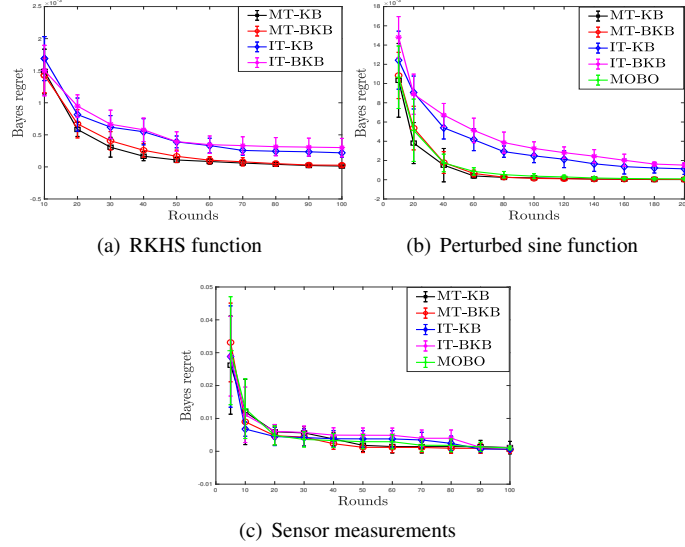


Figure 3: Comparison of Bayes regret of MT-KB and MT-BKB with IT-KB, IT-BKB and MOBO using Chebyshev scalarization.

**Comments on parameters used** We set the confidence radii (i.e.,  $\beta_t$  and  $\tilde{\beta}_t$ ) of MT-KB and MT-BKB exactly as given in Theorem 2 and Theorem 3, respectively. Similarly, for IT-KB and IT-BKB, we use respective choices of radii given in (Chowdhury and Gopalan, 2017) and (Calandriello et al., 2019) in the context of single task BO and suitably blow those up by a  $\sqrt{n}$  factor to account for  $n$  tasks. For MOBO, we use the UCB acquisition function and set the radius as specified in (?). To make the comparison uniform across all experiments, we do not tune any hyper-parameter for any algorithm and for a particular hyperparameter, we always use the same value in all algorithms. The hyper-paramter choices are specified in Section 5. We though believe that careful tuning of hyper-parameters might lead to better performance in practice.

**A note on the sensor data** The data was collected at 30 second intervals for 5 consecutive days starting Feb. 28th 2004 from 54 sensors deployed in the Intel Berkeley Research lab. We have downloaded the data previously from the webpage <http://db.csail.mit.edu/labdata/labdata>. But the link appears to be broken now. We can share a copy of our downloaded version if asked to do so.